October 2018

TARGETED LOCALIZATION OF MICROTUBULE-SEVERING ENZYMES TO CREATE NEW LOCAL TOOLS TO STUDY CELL DIVISION

Siddheshwari Advani

TARGETED LOCALIZATION OF MICROTUBULE-SEVERING ENZYMES TO CREATE NEW, LOCAL MICROTUBULE-DISRUPTION TOOLS TO STUDY CELL DIVISION

A Dissertation Presented

by

SIDDHESHWARI ADVANI

Submitted to the Graduate School of the

University of Massachusetts Amherst in partial fulfillment

of the requirements for the degree of

DOCTOR OF PHILOSOPHY

September 2018

Molecular and Cellular Biology Program

TARGETED LOCALIZATION OF MICROTUBULE-SEVERING ENZYMES TO CREATE NEW, LOCAL MICROTUBULE-DISRUPTION TOOLS TO STUDY CELL DIVISION

A Dissertation Presented

by

SIDDHESHWARI ADVANI

Approved as to style and content by:

_____
Jennifer L. Ross, Chair

_____
Pablo E. Visconti, Committee Member

_____
Thomas J. Maresca, Committee Member

_____
Peter Chien, Committee Member

_____
Scott Garman,
Director, Molecular and Cellular Biology Program

DEDICATION

To my grandfather, Dialmal Chetanram Sippy.

ACKNOWLEDGMENTS

Thank you to my advisor, Dr. Jennifer Ross, for one of the best Ph.D. experiences I've had. Her guidance, support, and faith in me allowed me to become independent very quickly in an interdisciplinary setting. Her dedication to science and teaching is inspirational. Thank you for giving me the opportunity to go to AQLM in May 2017. My goal - to put meaningful numbers on biological processes – remains the same.

Thank you to my committee members – Dr. Pablo Visconti, Dr. Tom Maresca, and Dr. Peter Chien for their infectious enthusiasm, insight, time, training, and guidance. Over the course of my Ph.D., this has extended to committee meetings, coursework, and journal clubs. It is my great pleasure to have been an honorary member of the Visconti lab; performed many of my experiments in the Maresca lab, and having spent my first lab rotation in the Chien lab.

Thank you to the UMass graduate school for a Dissertation Research Grant; Abveris for making me a custom anti-human katanin p60 antibody, ASCB and MBL for scholarships so that I could attend courses and conferences.

A big thank you to my dearest friends - Dr. Joe Torres, Dr. Joelle Labastide, Edwin Murenzi, Vanessa Martinez, and Madison Tyler. You continue to be my source of inspiration, reason, and strength. This is for the unforgettable Sunday night family-style dinners, impromptu kidnappings from campus, flowers, venting sessions, and celebrating my successes.

My time in the Ross lab has been a happy one because of amazing

colleagues and mentees such as Liudmila Belonogov, Madison Tyler, Austin Morrissey, and Bahar Rouhvand. I've learnt so much about physics and microscopy from Dr. Joelle Labastide, Dr. Vikrant Yadav, and Dr. Peker Milas. It has been such a joy working alongside them.

Thank you to my friends from the MCB and VASCI programs, namely Dr. Banyoon Cheon, Dr. Payal Yokota, Dr. Deborah Frenkel, Dr. Maria-Gracia Gervasi, Dr. Furkan Ayaz, Dr. Abla Tannous, among many others. My friends from other departments, namely Dr. Dirk Ruiken (Computer Science), and Dr. Brittany deRonde (Polymer Science and Engineering) – we've kept each other company during the writing process over numerous cups of coffee.

Other professor friends that I want to thank are – Dr. Ana-Maria Salicioni, Dr. Joe Jerry, Dr. Lisa Minter, and Dr. Pat Wadsworth. Your invaluable advice in both scientific and non-scientific matters has helped me chart my path.

To the Graduate Women In STEM – especially Dr. Joelle Labastide, Vanessa Martinez, Raquel Bryant, Dr. Rachel Koh, Madison Tyler, and Reilly Curtin - it has been a great honor serving as the Diversity and Inclusion Chair.

Thank you to my friends outside of academia - Alisha Allen, Risë and Amiana Banks, among many others.

Finally, thank you to my family – education has always been our highest priority. You push me to do better every day.

ABSTRACT

TARGETED LOCALIZATION OF MICROTUBULE-SEVERING ENZYMES TO CREATE NEW, LOCAL MICROTUBULE-DISRUPTION TOOLS TO STUDY CELL DIVISION

SEPTEMBER 2018

SIDDHESHWARI ADVANI

B.Sc., ST. XAVIER'S COLLEGE, UNIVERSITY OF MUMBAI, INDIA

M.Sc., UNIVERSITY OF HYDERABAD, INDIA

Ph.D., UNIVERSITY OF MASSACHUSETTS AMHERST, USA

Directed by: Professor Jennifer L. Ross.

Microtubules are polymeric protein filaments made of the monomeric alpha-beta tubulin heterodimer. They are important for physical attributes of the cell such as shape and structure, and drive essential processes such as cell division, cell migration, and active transport of metabolites. This occurs through the control of microtubules in space and over time through the lifetime of the cell. The shape and interior rearrangements are created by a diverse group of microtubule-associated proteins. When this regulation goes awry, microtubules location, stiffness, and structure are compromised, which is what is seen in diseases such as Alzheimer's. Multiple microtubule networks can exist within a

single cell under distinct spatiotemporal regulators. These networks remain poorly studied because current methods to disrupt the microtubule cytoskeleton do not easily provide rapid, local control with standard cell manipulation reagents. Here, we develop a new microtubule-disruption tool based on katanin p60 severing activity and demonstrate proof-of-principle by targeting it to kinetochores in *Drosophila melanogaster* S2 cells. Specifically, we show that human katanin p60 can remove microtubule polymer mass in S2 cells and an increase in misaligned chromosomes when globally over-expressed. When targeted to the kinetochores via Mis12, we were able to recapitulate the misalignment only when using a phosphorylation-resistant mutant. Our results demonstrate that targeting an active version of katanin p60 to the kinetochore can reduce the fidelity of achieving full chromosome alignment in metaphase and could serve as a microtubule disruption tool for the future.

TABLE OF CONTENTS

Page

LIST OF FIGURES

Figure Page

CHAPTER 1

INTRODUCTION

1.1 What are microtubules?

Microtubules are an integral part of the cellular architecture and transport machinery. They are composed from alpha and beta tubulin heterodimers linked non-covalently into long filamentous arrays rolled into a hollow tube. Microtubules are exhibit dynamic behaviors and can be acted upon by microtubule-associated proteins and regulators. This allows the microtubule network to change during various cellular processes in response to external cues. In several cellular processes, microtubules coordinate with the actin cytoskeleton to carry out functional changes in the cell.

1.2 Inherent properties

The properties of microtubules must be considered in order to understand the biochemical properties that can be modulated, for these polymeric proteins to participate in diverse cellular processes. Microtubules can switch between shrinking and growing phases, a process called dynamic (Mitchison & Kirschner, 1984). This is because they have intrinsic GTPase activity that phosphorylates GDP to GTP, leading to dissociation of tubulin from the microtubule polymer. The dynamic nature is regulated at multiple levels by many post-translational modifications, microtubule associated proteins and enzymes. These accessories control aspects such as stability, location, stiffness, and affinity for other cellular

components. Microtubule-severing enzymes are one regulatory mechanism of the cytoskeleton.

1.3 Multiple distinct microtubule networks exist within cells

The cell has an inherent capability to provide local control of the microtubule network, at each distinct location of the cell, spatially separated by 10 to 1000 μm depending on cell type, becoming mechanically and chemically distinct. The chemical and physical properties of the microtubule network in each location depends on cell type, stage in the cell cycle, or development. One particularly important role of microtubules occurs during mitosis. Even within this single process, microtubules display differential localizations, dynamics, and signaling. Astral microtubules help to keep the spindle localized within the cell volume (Kern et al., 2016; Pease et al., 2011; Giansanti et al., 2001). Kinetochore microtubules connect, localize, and apply forces to kinetochores to establish aligned chromosomes in metaphase (Waters, 1996; Maiato et al., 2004; Elting et al., 2017). Another set of microtubules that could either be a dense cloud of aligned, short filaments or overlapping interpolar filaments, fill in around the kinetochore microtubules (recently reviewed in Orieola et al., 2018). Despite the spatial overlap of these networks, they are still controlled locally. Such exquisite control highlights a need to be able to manipulate microtubules in a targeted manner, spatially and temporally. This is especially seen in neurons, where the regulation of the different compartments occurs in distinct manners, as shown in Figure 2.

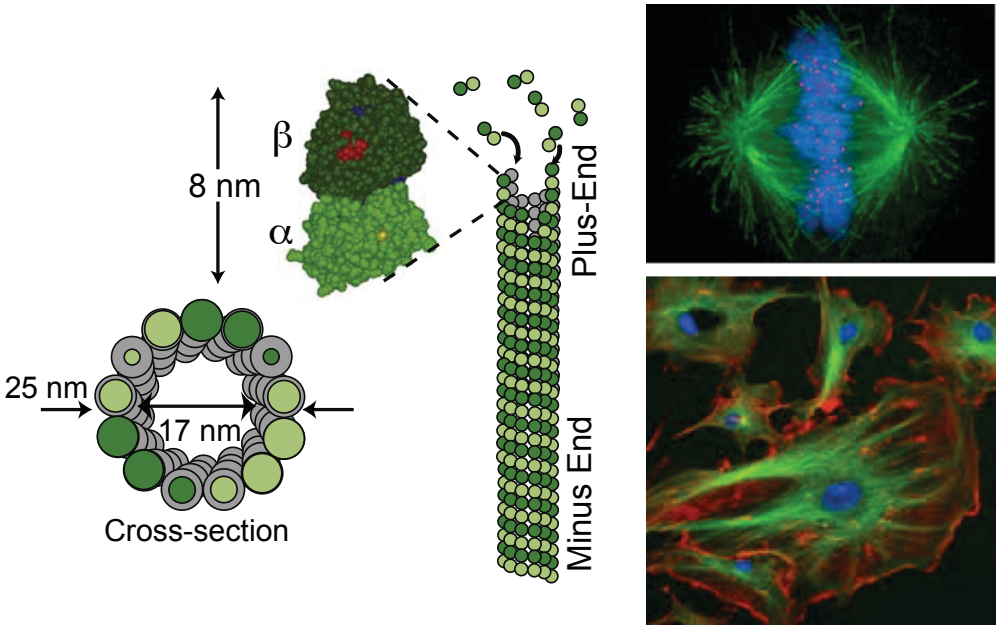

Figure 1: Cartoon of Microtubule structure and organization during mitosis and cell migration

Cartoon representation of alpha and beta tubulin subunits in their head-to-tail filamentous organization to form a microtubule, shown in (A) from Hawkins et al., 2010. Images of GFP-microtubules for mitotic (B) and migrating cells (C) were obtained from Wikipedia.

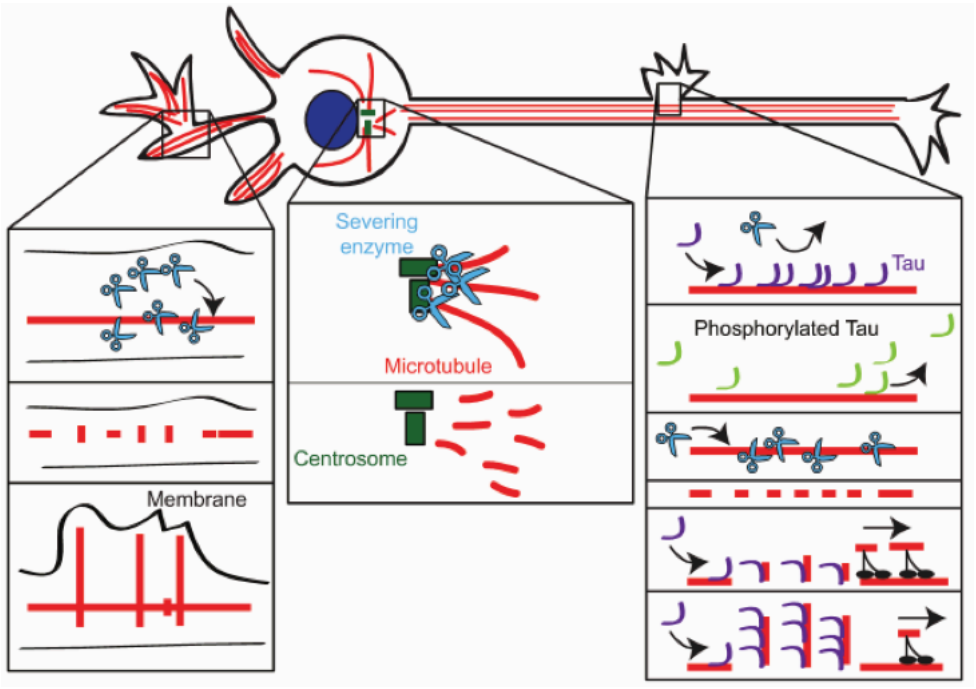

Figure 2: Cartoon of microtubule regulation in spatially distinct networks in a neuron

An example of distinct modes of microtubule regulation within a single cell. Note that the regulation of microtubule nucleation and severing is under control of microtubule-severing enzymes such as katanin p60 and spastin. Figure referenced from Sharp and Ross, 2012.

1.4 Microtubule-severing enzymes

One family of accessory proteins is the meiotic clade of ATPases Associated with diverse cellular Activities (AAA), and comprises of spastin, fidgetin, katanin, and Vps4 and their isoforms (Frickey & Lupas, 2004). The group is named after the meiotic functions of the *C. elegans* homologs of katanin p60 (mei-1) and p80 (mei-2). Katanin was first identified by McNally and Vale as an ATP-driven microtubule-severing enzyme (McNally & Vale, 1993). McNally and Thomas found through immunodepletion experiments in *Xenopus* oocytes that katanin was required during mitosis and makes a major contribution to M-phase severing activity (McNally & Thomas, 1998). Expression of katanin was also seen in *Xenopus* A6 cells, human fibroblasts and the brain (McNally & Thomas, 1998). These enzymes may have co-factors or domains for cellular targeting; katanin p80 targets katanin p60 to the centrosome (Hartman et al., 1998); and the M1 isoform of Spastin has a membrane-tethering hydrophobic domain, unlike the rest of the meiotic clade (Salinas et al., 2005). Fidgetin-like 1 has a Nuclear Localization Signal, however, has not been extensively studied compared to katanin and spastin (Yang et al., 2005).

1.5 Structure and mechanism of microtubule-severing enzymes

Katanin, fidgetin, spastin and their isoforms share a common domain architecture consisting of an N-terminal microtubule interacting and trafficking (MIT) domain and a C-terminal AAA ATPase domain (Vale, 2000). Microtubule binding of katanin is ATP- dependent and facilitates monomer-monomer interactions (Hartman & Vale, 1999). Recently, the X-ray crystal structure the

katanin p60 monomer from *C. elegans* was solved by Zehr et al. (2017), and the data used to solve the cryo-EM structure of the hexamer. There are known crystal structures for spastin, Vps4 and fidgetin-like 1 exist in the PDB database (Han et al., 2015; Monroe et al., 2014; Peng et al., 2013; Roll-Mecak & Vale, 2008). From the experimentally-confirmed data obtained for other hexameric AAA ATPases, it has been proposed that severing enzymes cut through threading the CTTs of tubulin through the hexamer pore (Roll-Mecak & McNally, 2010; Roll-Mecak & Vale, 2008; Sharp & Ross, 2012). There are two possible, non-mutually exclusive mechanisms. The severing enzyme could couple ATP hydrolysis with unfolding of the tubulin dimer to remove it (Zehr et al., 2017). Or, the enzyme could wedge out the dimer. Of course, both mechanisms could also occur.

1.6 Broad relevance of microtubule-severing enzymes in the context of cellular compartments studied so far, and their role in disease

There has been an increasing focus on microtubule-severing enzymes because of their roles in disease, cell division, maintenance of axon terminals, and migration, as covered by several reviews (Monroe & Hill, 2016; Sharp & Ross, 2012). For fidgetin, spastin and FL2, therapeutic applications have been suggested, explored and patented (Charafeddine et al., 2015). Here, we focus on the roles of katanin p60 during a multitude of cellular processes, as described in further sections.

1.7 How does katanin promote cell division?

Katanin p60 is required at the midzone, and the destabilization of the microtubules at the midzone is needed for furrow ingression so that daughter cells can separate. Its inhibition via siRNA leads to incomplete cytokinesis by stabilization of microtubules that form the central spindle (Matsuo et al., 2013). An increase in binucleated cells and apoptotic cells is seen relative to the control siRNA-treated cells (Matsuo et al., 2013).

1.8 Roles of katanin during cell migration

We still do not know the mechanism behind the observation that the loss of katanin leads to an increase in cell migration, beyond the persistence of microtubules (Charafeddine et al., 2015; D. Zhang et al., 2011). Drosophila D17 cells knocked down for katanin p60 via siRNA show an increase in cell migration relative to the control siRNA treated cells (Zhang et al., 2011). A similar effect was observed for human Fidgetin-Like 2 (Charafeddine et al., 2015). This could be occurring through persistence of longer microtubules at the cell cortex in the absence of katanin p60 (Zhang et al., 2011). We do not know what localizes katanin p60 to the cell cortex; it lacks a membrane-binding domain, and known targeting factors of katanin p60 do not localize to the cortex. This is pertinent because katanin p60 has been implicated in many bone metastatic cancers. Katanin p60 overexpression is found in bone metastasis of prostatic cancer, and breast cancer cells (Fu et al., 2018). Insight into the mechanisms that regulate katanin activity during migration, and distinctions between the roles at the

leading-edge v/s the Golgi and other organelles, would allow us to develop tools to suppress cell motility in these cancerous cells.

1.9 Outstanding questions in the field

1.9.1 How are microtubule-severing enzymes targeted to cellular compartments and regulated there?

We do not know how the severing enzymes are targeted in the cell. For example, there are contrasting reports on the localization of transiently expressed Fidgetin and FL2. Yang and colleagues report that Fidgetin-GFP localized to the nucleus and was excluded from the nucleolus in transfected NIH3T3 mouse fibroblast cells (Yang et al., 2005). They also identified a bipartite nuclear localization signal for Fidgetin through deletion analysis. The same localization pattern is seen in Cos7 monkey kidney cells and HeLa human cervical epithelial cells for all three fidgetin homologs (data not shown in the paper) (Yang et al., 2005). FL2 shows predominantly nuclear localization like that of Fidgetin (Yang et al., 2005). However, endogenous FL2 shows cortical staining in U2OS cells (Charafeddine et al., 2015).

We know that over-expression of katanin itself leads to severing of microtubules in RFL-6 cells. Large-scale destruction of microtubules prevents us from obtaining meaningful information about the change in microtubule dynamics. Therefore, it becomes important to use an inducible system of expression where high local concentrations of severing enzymes can be obtained. Identifying direct regulators of function may be difficult due to transient association of severing enzymes. The ability to target these proteins to axon

terminals, leading and lagging edge of migrating cells, Golgi and spindle apparatus will allow for tighter spatial control and better resolution of their effects.

1.9.2 Roles of katanin during cancer

Reports of a role for katanin p60 in metastatic cancers have been identified by many groups. Katanin p60's role in prostate cancer bone metastasis was identified because of the differential expression between healthy and cancerous cells. In prostatic cancer, the basal cells are entirely absent and katanin expression is seen in the prostatic cancer cells (X. Ye et al., 2012). After these reports, katanin expression was looked at during breast cancer bone metasis (Fu et al., 2018). Immunostaining of katanin revealed enlarged areas of expression, and an increase in total katanin staining for both primary breast and bone metastatic cancers, over the control normal breast glands (Fu et al., 2018). The authors found decreased proliferation in triple negative MDA-MB-231 and MCF-7 cells expressing p60 from pCDNA 3.1 plasmids (Fu et al., 2018). These were substantiated by the complementary findings that cell migration was increased (Fu et al., 2018). Knockdown of katanin via shRNA increased cell proliferation and decreased migration in both cell lines (Fu et al., 2018). This finding contrasts with the findings from the Sharp lab that human katanin p60 played no role in cell migration (D. Zhang et al., 2011). Thus, an area of interest that remains ripe for investigation is how katanin severing activity can be modulated remains in cancerous cells. Treatment of lung cancer cells with purine-type compound called 5c was found to bind to katanin p60 and decrease tumor mass by increasing microtubule fragmentation (Kuo et al., 2016). This resulted in cells

arrested at the G2/M phase, and consequently driven down the mitochondrial apoptosis pathway (Kuo et al., 2016). Increased phosphorylation of c-Jun, a marker of apoptosis, was observed by western blots (Kuo et al., 2016). It is therefore not surprising that we have observed difficulties in obtaining stable S2 cell lines overexpressing katanin that still demonstrate microtubule destruction. However, decreased cell proliferation comes hand in hand with increased cell migration. While this could serve as a promising treatment for cancers that do not become metastatic, the compound does not bind to its target with the specificity needed in the nanomolar range, and would not discriminate between healthy and cancerous cells (Kuo et al., 2016).

1.9.3 Regulation of severing enzymes during mitosis

Another layer of katanin p60 regulation is via post-translational modifications. A number of phosphorylation sites have been predicted for katanin p60 (Loughlin et al., 2011). One of these phosphorylation sites was experimentally validated in a cross-species study by Loughlin et al (Loughlin et al., 2011). They showed that Aurora B kinase-mediated phosphorylation of Serine 131 on *Xenopus laevis* katanin p60 negatively regulates severing activity, thus acting as an additional means of control (Loughlin et al., 2011). Many other phosphorylation sites have been found for other katanin homologs and in different cellular contexts (Whitehead et al., 2013; Dixit lab and others).

1.10 Methods to manipulate the cytoskeleton

Currently, methods to disrupt cellular microtubules at a particular location and time are limited and technically challenging. For instance, a number of spindle poisons act in distinct ways to alter the dynamic instability of the microtubule polymer and are frequently employed in anti-cancer therapies (extensively reviewed in Jordan and Wilson, 2004). These pharmacological agents either stabilize or inhibit all the microtubules in the cell. Taxol stabilizes the microtubule cytoskeleton against depolymerization (Arnal and Wade, 1995). Vinblastine destabilizes the microtubule network by binding to tubulin dimers and inhibiting their incorporation into filaments (Gigant et al., 2005; Panda et al., 1996). These pharmacological methods, while useful in grossly perturbing the microtubule cytoskeleton, are limited in their ability to modify microtubules locally. Physical perturbations that are non-pharmacological include laser ablation. This method is technically challenging enough to be limited to a small group of expert laboratories. Further, laser ablation must be finely controlled and tuned to not damage other cellular structures and processes. Laser ablation is also limited to a small set of cell types. Therefore, existing methods are limited in their ability to give us information about the spatially distinct cytoskeletal networks.

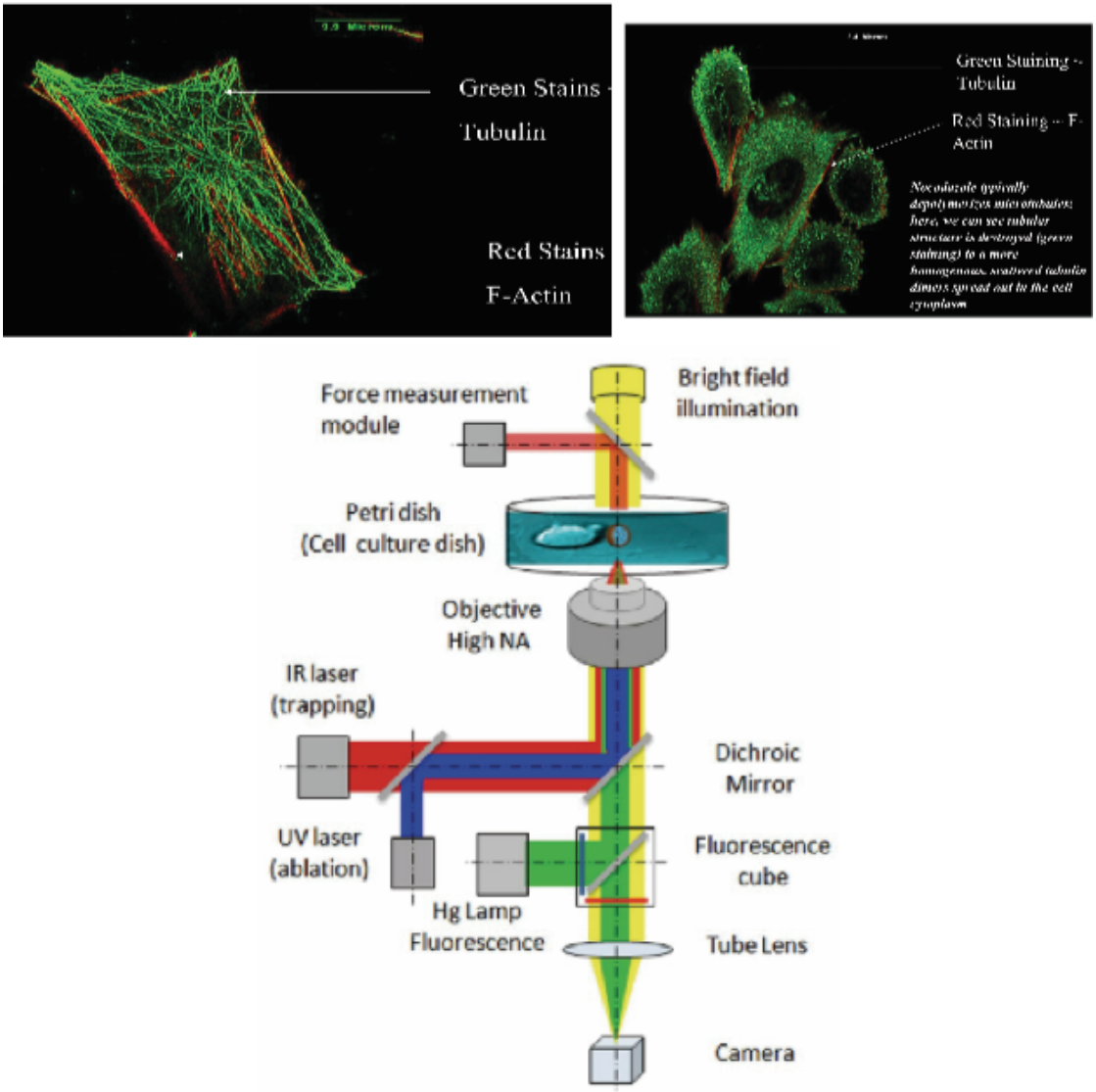

Figure 3: Pharmacological methods and laser ablation tools for microtubule disruption.

Pharmacological methods such as taxol and nocodazole affect the entire cytoskeleton and lack precise control. On the other hand, laser ablation is not well-suited for high throughput experiments and requires additional modification of existing setups to work.

1.11 Project goals

In this dissertation, we aim to develop tools to manipulate the cytoskeleton so that we can study local microtubule dynamics. The properties of katanin p60 make it a potentially useful microtubule-control tool.

For instance, Bailey et al. have previously shown that the severing activity of katanin p60 is inhibited by high concentrations of free tubulin (Bailey et al., 2015). This result implies that a high concentration of katanin p60 is needed locally to elicit severing activity, and the subsequent release of large amounts of free tubulin dimers will turn off further severing activity. This provides an internal negative feedback loop to shut down severing after significant polymer loss. Specifically, high concentrations of katanin p60 will need to be localized to a specific region, but the disruption we want to obtain should be acute; not long term. This is important for visualizing both chemical and spatial regulation.

1.12 Project scope

Here, we want to test the abilities of this novel microtubule-disruption scheme in a location of interest where katanin p60 is thought to function, yet its role might not be immediately clear. We picked the kinetochore because it has been hypothesized that katanin p60-mediated destruction of microtubules precedes kinesin-13-mediated depolymerization of kinetochore fibers at anaphase onset (Zhang et al., 2007). However, immunofluorescence data shows that katanin p60 is around the chromosomes in Drosophila S2 cells, but no staining marker for kinetochores is shown (Zhang et al., 2007). Immunofluorescence data from

Xenopus laevis and *Xenopus tropicalis* show staining of katanin at the metaphase plate (Loughlin et al., 2011). Mis12 is a component of the Mis12 complex, that, together with the Ndc80 complex and KNL1 comprise the KMN network that mediates kinetochore interaction with spindle microtubules (Venkei et al., 2012). It was thought that k-fiber attachments to spindle poles was essential for chromosome segregation during anaphase, however, two distinct mechanisms seem to be operating. There is evidence for a role of katanin p60 in depolymerization of microtubules at the plus ends, a process called Pacman flux ((Zhang et al., 2007). There is evidence for spastin and fidgetin to be participating in minus end depolymerization of microtubules at centrosomes, a process that gradually leads to poleward flux of chromatids (Zhang et al., 2007). The molecular switch that initiates Pacman flux is not known but is suspected to occur upon relaxation of tension between the kinetochores. In the absence of K-fiber attachments to the spindle pole, chromosomes can still be transported to the poles via a dynein-mediated process (Sikirzhytski et al., 2014). The process also appears to be sensitive to inhibitors of actin and myosin, as determined in crane fly spermatocytes, but a mechanism has yet to be elucidated (Forer et al., 2007). This is discussed in further detail in a review by Forer et al. (2015).

It has been previously shown that Mis12 could be modified with fusion proteins while still localizing and functioning at the kinetochore (Ballister et al., 2014; Maldonado & Kapoor, 2011; Ye et al., 2015). Further, Mis12 localization to the kinetochores was microtubule-independent (Kline et al., 2006; Venkei et al., 2012). Thus, if the katanin p60 locally destroyed the microtubules, I would expect

that the Mis12 and katanin p60 would still reside at the kinetochore. Finally, Mis12 constitutively associated with centromeres throughout the cell cycle in *Drosophila* cells so Mis12-katanin p60 should localize to the nucleus during interphase (Kline et al., 2006; Venkei et al., 2012).

We show that our new katanin-based tool can be successfully localized to the *Drosophila* kinetochore and remains active there. Specifically, we have created a copper-sulfate inducible fusion construct with a fluorescent protein, TagRFP-T, for chemical induction and to visualize localize katanin p60 to the kinetochore via fusion with Mis12, and quantify effects seen at the kinetochore due to katanin activity.

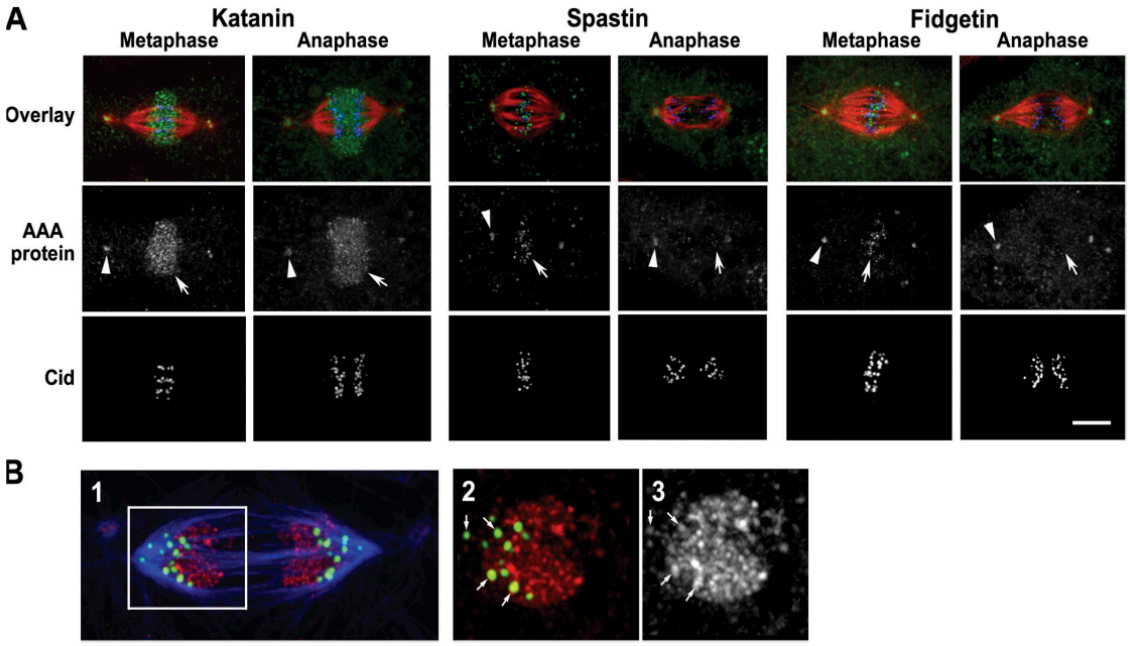

Figure 4: Immunofluorescence localization of katanin p60, fidgetin, and spastin in S2 cells in mitosis.

Microtubule-severing enzymes play important roles in Drosophila S2 cell mitosis. Shown in (A) is staining for katanin, fidgetin, and spastin during metaphase. Cid is a Histone H3-like centromeric protein. All the severing enzymes localize to the centrosome and around the chromosomes. Magnification of immunofluorescence during anaphase for katanin p60, depicted in red, in proximity to Cid (green) and microtubules (blue). Adapted from Zhang et al., 2007.

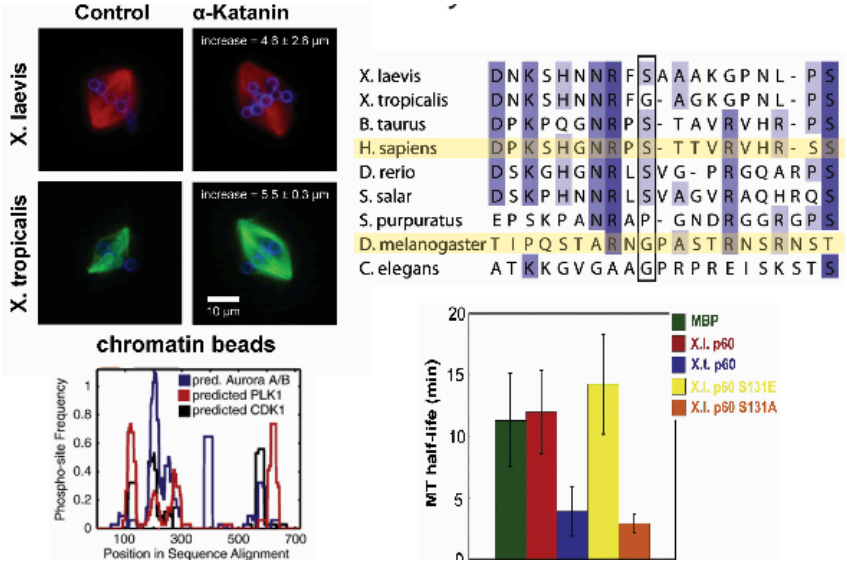

Figure 5: Phosphorylation of Serine 131 on katanin p60 by Aurora B kinase acts an an off-switch for severing activity.

(A) Chromatin-coated beads were incubated with egg extracts from *Xenopus laevis* and *Xenopus tropicalis* and immuodepleted using a no-antibody control or anti-katanin p60. (B) Predicted phosphorylation sites in the N-terminal MIT domain of Drosophila p60. (C) Sequence alignment of Ser131 phosphosite conservation in vertebrates. (D) Flow-cell destabilization assays using X.laevis egg extracts supplemented with MBP-tagged proteins measure microtubule half-life, a stability parameter (the concentration of microtubules is not reported). Adapted from Loughlin et al., 2011.

CHAPTER 2

METHODS

2.1 Generation of constructs to express katanin p60 in S2 cells

Human katanin p60 was cloned from pMal-c2x MBP superfolder GFP human katanin (Bailey et al., 2015) into pMT-V5 His B TagRFP-T DmMis12 via Gibson cloning (Gibson, 2011) using the EcoRI site, generating pMT-V5 His B TagRFP-T DmMis12 HsKatanin p60 (TagRFP-T Mis12 katanin p60). The S131A mutation was made via site- directed mutagenesis using a modified version of the QuikChange XL protocol (TagRFP-T Mis12 katanin p60 S131A) (Qi & Scholthof, 2008).

2.2 Transient transfection of S2 cells

Transient transfections of S2 cells were performed in a GFP-tubulin background using the Qiagen Transfection kit (Qiagen). GFP-tubulin S2 cells were plated at high density one hour prior to transfection in a 35 mm tissue culture dish. Briefly, 1 µg of DNA was diluted with Buffer EC in a microfuge tube to obtain a final volume of 300 µl. This was mixed with 16 µl of Enhancer and incubated for 5 minutes. At the end of the incubation period, 60 µl of Effectene was added to the mixture and incubated for 10 minutes. One milliliter of complete S2 media was added to the tube, pipetted to mix, and added dropwise, replacing the existing S2 media in the dish. The dish was sealed with Parafilm and incubated at 24^{o}C. The next day, 1 ml of complete media was added to the dish and sealed with Parafilm. On day 3, a small sample of cells were induced overnight with 500 µM $CuSO_4$. Cells were inspected for transfection efficiency

and imaged on day 4. The remainder of the uninduced cells were transferred to a new flask and treated with 25 µg/ml blasticidin. Each round of selection was evaluated after induction, and when no further increase in the ratio of expressing to non-expressing cells was seen, the cells were taken out of selection to make cryo-preserved stocks. Typically, each cell line undergoes 3-4 rounds of selection, however, we were not able to obtain stable cell lines expressing soluble p60WT or soluble p60S131A.

2.3 Misaligned Chromosome Assay

2.3.1 Sample preparation and image acquisition

Stable or transiently transfected S2 cell lines were induced with 500 µM $CuSO_4$ overnight. Acid-washed coverslips were sterilized and coated with ConA. The cells were plated onto ConA-coated coverslips placed in 35 mm dishes for 30 minutes at 50% confluency, treated with 20 µM MG132 in fresh S2 media for 1 hour, and subsequently processed for immunofluorescence.

2.3.2 Immunofluorescence

Coverslips were washed twice with BRB-80, fixed with 10% paraformaldehyde for 10 minutes, and permeabilized with PBS 1% Triton X-100 for 8 minutes. This method was used because it was the best at preserving the microtubule organization and the TagRFP-T signal. Coverslips were subsequently rinsed thrice with PBS 0.1% Triton X-100 and transferred onto a Parafilm sheet placed in a 150 mm dish. The coverslips were blocked with 5% Boiled Donkey Serum in PBS for 45 minutes. For most assays, we used primary

antibodies to anti-a tubulin antibody (DM1alpha, Millipore) only. For examination of tubulin, katanin, and TagRFP-T localization, we used anti-GFP (Millipore), anti-TagRFP-T (Evrogen) and anti- human katanin p60 (Abveris). Primary antibodies were diluted in Boiled Donkey Serum at 1:1000 (DM1alpha or GFP), 1:5000 (anti-TagRFP-T), or 1:50 (anti-human katanin p60) and incubated with the coverslip for 1 hour at room temperature. The coverslips were washed thrice for five minutes each in PBS 0.1% Triton X-100, incubated with secondary antibodies diluted in Boiled Donkey Serum for 40 minutes to 1 hour, and washed again in the same manner with PBS 0.1% Triton X-100. The coverslips were stained with DAPI at a final concentration of 1 µg/ml in 5% Boiled Donkey Serum and washed thrice for 5 minutes each with PBS 0.1% Triton X-100. The coverslips were mounted in a glycerol-based Mounting Media and sealed with nail polish. The slides were stored at 4^{o}C. TagRFP-T fluorescence was preserved in this manner for up to three weeks.

2.3.3 Scoring

A Nikon Ti Eclipse widefield microscope was used to visualize DNA using DAPI (405 nm), GFP-tubulin or secondary antibody on immunostained tubulin (488 nm), and TagRFP-T (561 nm). Cells were scored as misaligned if their chromosomes were more than 50% of the distance between the spindle pole and the metaphase plate. As is common with S2 cell cultures, ~50% of the cells do not express the protein of interest and provide an internal control for our experiments.

2.3.4 Statistical analysis

The misaligned chromosome counts are discrete data with an integer number of misaligned chromosomes per cell. Histograms of the misaligned chromosome data for both katanin p60-expressing and non- expressing cells yield non-Gaussian distributions that cannot be evaluated using the student's t-test. Hence, we used the Chi-square test to evaluate statistical significance. The degrees of freedom were calculated to be 1, and the Chi-square value was evaluated and compared to the expected Chi-squared value at p=0.05, p=0.01, and p=0.001 significance levels. Chi-squared tests required that the number of cells in the control and experimental populations be equivalent. Often, the number of control cells was higher than those expressing. To compare the data, we rescaled the number of control cells both with and without misaligned chromosomes, so that the total number of control cells in the comparison population equaled the number of expressing cells measured (https://www.graphpad.com/quickcalcs/chisquared1.cfm).

2.4 Quantification of microtubule polymer

2.4.1 Sample preparation and image acquisition

Cells were induced as described previously and plated at 50% confluency on ConA-coated, glass bottomed petri dishes (MatTek) for 20 min. Fresh pre-warmed media was added to the dish, and subsequently imaged on a spinning disk confocal microscope (Nikon Ti Eclipse) using a 100x oil immersion objective NA=1.49, at 2x2 binning and 0.2 μm Z-steps (ORCA Flash 4.0). Live cells were visualized for GFP-tubulin using the 488 nm laser and TagRFP-T using the 561

nm laser. The exposures chosen for each of these wavelengths were 100 ms for the 488 nm laser, and 300 ms for the 561 nm laser, to minimize bleaching of the cells. The dish was imaged for a maximum of 1 hour. Chosen cells were well-separated from their neighbors, and a z-stack of images was taken to span the entire depth of the cell for both GFP and TagRFP-T channels (Figure 8). The z-stack was used to create maximum projection images and reveal the location of the nucleus. Quantification in live cells was preferred because fixed cells displayed more background than live cells.

2.4.2 Image quantification

Files were imported into FIJI/ImageJ, and a maximum projection of the z-series was obtained for both channels (GFP-tubulin and TagRFP-T). To select only the microtubules in the field of view, the GFP channel was auto-thresholded and adjusted if needed to include the entire outline of the cell area. The Particle Analyzer command was run to add the thresholded areas to the region of interest (ROI) manager, generating outlines of the cells. Partial and conjoined cells were eliminated from the measurements. The ROI was used to measure the total area and total intensity of 16-bit, un-thresholded cells in the RFP channel. To measure the TagRFP-T signal in each cell, the TagRFP-T threshold was set to eliminate the background signal outside the cell and was found to be fairly constant across all images. The cell outline ROIs obtained from the GFP channel were transposed onto the TagRFP-T max projection to measure the TagRFP-T area and intensity. The thresholded image revealed the TagRFP area and intensity

above background noise, and the un-thresholded image gave the TagRFP intensity and area of the entire cell.

2.4.3 Statistical analysis

The normalized microtubule polymer mass and TagRFP-T signal were continuous variables between zero and one. Histograms of the data were not Gaussian distributions, so the student's t-test should not be used. We ran the Kolmogorov-Smirnov test to determine if the two distribution sets are statistically different. (http://www.physics.csbsju.edu/stats/KS-test.html). We determined the maximum difference between the cumulative distributions D, and compared this to the expected value of D at a given significance. If the distribution sets were found to have a D value smaller than the critical value of D at p=0.05, then the null hypothesis was accepted. If the two distribution sets had a D value larger than the critical value of D at p=0.05, we would reject the null hypothesis. Further, we used the Wilcoxon-Mann-Whitney test to evaluate the statistical significance of the data between expressing and non-expressing cells.

2.5 Detection of Mis12p60 localization by immunofluorescence

2.5.1 Sample preparation for immunofluorescence assay

Fixed cells were visualized for GFP-tubulin and TagRFP-T by plating induced cells on ConA-coated coverslips. Cells were immunostained with anti-a tubulin antibody (DM1a, Millipore) followed by green secondary antibody to mouse (Alexa-488, 488 nm).

2.5.2 Imaging

TagRFP-T was imaged directly or stained with anti-TagRFP-T antibody followed by red secondary antibody to rabbit (Alexa-561, 561 nm). The exposures chosen for each of these wavelengths were 200 ms for the 488 nm laser, and 500 ms for the 561 nm laser. The coverslip was imaged within 1 week. Chosen cells were well-separated from their neighbors, and a z-stack of images was taken to span the entire depth of the cell for both GFP and TagRFP-T channels (Figures 5-8). Fixed cells displayed more background than live cells, and were only used to demonstrate (A) co-localization between TagRFP-T and katanin p60, or (B) identify cells that expressed katanin for the unlabeled katanin control (Figure 9).

CHAPTER 3

OVEREXPRESSION OF EXOGENOUS HUMAN KATANIN P60 WT AND S131A IN DROSOPHILA S2 CELLS

3.1 Summary

In this chapter, I describe the effects of globally overexpressing human katanin p60 in a model system, *Drosophila* S2 cells, to determine if there is an effect on local destruction of microtubules during interphase, and examine mitotic phenotypes such as spindle length, intra-kinetochore distance, chromosome misalignment, and mitotic duration. This would confirm if our human protein was able to work in the *Drosophila* system, and we would expect to see many of the phenotypes that could be caused by katanin overexpression. I was unable to obtain stable cell lines expressing WT or S131A p60, and consequently had to use transiently transfected cells. I found that spindle length, intra-kinetochore distance, and mitotic duration were not significantly affected, but there was a significant increase in chromosome misalignment for both the wildtype and the Aurora B kinase phosphorylation-resistant mutant Serine 131 Alanine (S131A) katanin p60. Analysis of the chromosome misalignment between wildtype p60 and S131A p60 showed that the increases for cells expressing these proteins are within the uncertainty range of each other.

3.2 Introduction

In interphase, the over-expression of *Drosophila* katanin p60 can remove the microtubule polymer mass in a dose-dependent manner (Zhang et al., 2007; Grode and Rogers, 2015). However, little was known about the regulation of

katanin during mitosis. The Heald group reported a difference in spindle sizes for *Xenopus laevis* (the larger of the two species) and *Xenopus tropicalis* and attributed the differences to Aurora B kinase-mediated regulation of katanin p60 (Loughlin et al., 2011). The serine residue phosphorylated by this kinase at position 131 is present in *Xenopus laevis* but absent in *Xenopus tropicalis*. The Heald group reported that the wildtype version has a higher microtubule-stimulated ATPase activity than the phosphomimic S131E (serine to glutamate) variant. We were expecting to see a significant difference in spindle length upon overexpression of the human protein in *Drosophila* S2 cells (Whitehead et al., 2013) but did not make such observations.

It has been shown by many groups that human katanin p60 shows microtubule-severing activity *in vitro* (Bailey et al., 2015). However, many factors prevent it from being used directly as a tool to obtain localized microtubule-severing *in vivo*. Most studies on katanin have utilized transient transfection to examine phenotypes because stable cell lines are difficult to obtain in several cell types. Indeed, this is what I observed when trying to obtain stable cell lines for katanin p60 and saw that well-documented phenotypes on microtubule polymer loss were subsequently lost upon increasing the concentration of the selection drug, and over multiple rounds of selection. It is important to have an inducible system so that a range of expression levels of soluble katanin can be compared to that of tethered katanin in a specific cellular compartment (Figure 4). We first needed to determine if human katanin p60 could act on *Drosophila* microtubules to disrupt the interphasic microtubule network. If functional, we expected that

overexpression of the soluble human katanin p60 in S2 cells would lead to a decrease of *Drosophila* microtubule polymer mass. If katanin p60 was widely affecting the process of mitosis, several phenotypes would have been observed including misaligned chromosomes, spindle length changes, large scale spindle disorganization, or anomalous positioning of the spindle.

3.3 Results

3.3.1 Human katanin p60 WT is active in Drosophila S2 cells and decreases MT polymer

I performed experiments with transient transfections of globally expressed TagRFP-T katanin p60 in S2 cells in a GFP-α-tubulin background (Figure 7), and imaged live cells in the GFP-microtubule polymer and TagRFP-T katanin p60 channels using a spinning disc confocal microscope. I subsequently quantified the levels of microtubule polymer mass and TagRFP-T expression, as described in the Methods. Using maximum projection of z-stack images of live cells (Figure 7A-C), I measured the area occupied by high-intensity GFP-microtubule polymer and the TagRFP-T signal and normalized each to the total area of the cell. The microtubule polymer density (y-axis) was plotted as a function of TagRFP-T expression (x-axis) on a scatter plot for all cells (Figure 7D). For non-expressing cells, the TagRFP-T signal consistently registered the same intensity as background levels, which is shown on the left side of the plot (Figure 7D, red boxes). Cells expressing TagRFP-T katanin p60 wildtype had a significantly higher katanin p60 concentration and were consistently on the right side of the plot (Figure 7D, blue circles). I took the TagRFP-T data and plotted them using a

box-whisker plot to demonstrate that there was significantly more katanin in the expressing cells (Figure 7E, $P < 0.0001$).

The distribution of the microtubule density fraction for non-expressing and expressing cells were plotted as box-whisker plots and were observed to have significantly different distributions, with the mean and median significantly lower for the cells expressing TagRFP-T katanin p60 wildtype (Figure 7F). We used Kolmogorov-Smirnov (KS) and Wilcoxon-Mann-Whitney statistical tests and found that the polymer mass for expressing and non-expressing cells are distinct ($P < 0.0001$). These results are consistent with an interpretation that the TagRFP-T katanin p60 can actively reduce microtubule polymer and is capable of severing and/or depolymerizing *Drosophila* microtubules in S2 cells.

We noted that some of the cells expressing high levels of TagRFP-T katanin p60 appeared to display aggregates of katanin. In all these cases, the background level of katanin was also relatively high, and the microtubule density was low. Such katanin aggregates were observed in a prior study that overexpressed *Drosophila* katanin in S2 cells (Zhang et al., 2007), and are likely a result of overexpression of a labeled katanin. In this prior study, cells displaying aggregates also showed reduced microtubule polymer mass (60% reduction) on average (Zhang et al., 2007). My experiments demonstrate a 94% reduction of the microtubule polymer mass which is consistent with prior results. Although this prior study showed that cells with aggregates were able to reduce the microtubule polymer mass (Zhang et al., 2007), the intensity settings for the

images published in that manuscript made it difficult to determine if there was a soluble pool of katanin in addition to aggregates.

3.3.2 Soluble human katanin p60 leads to misaligned chromosomes in mitosis

There were no gross changes in the mitotic spindle length or morphology when human katanin p60 WT was overexpressed in S2 cells, which was contrary to our expectation (Figure 11A-D). However, there was an increase in the percentage of MG132-treated cells with >1 misaligned chromosome when WT katanin p60 was overexpressed globally. We found that 20 ± 3% of the overexpressing cells had misaligned chromosomes compared to 6 ± 1% in control cells not expressing the construct in the same chamber (Figure 11E). This 3.5 ± 0.9-fold change was significantly above 1. (Figure 11F) implying that over-expressed soluble human katanin p60 could alter mitotic microtubule dynamics in a manner that did not dramatically change spindle morphology, but did lead to a higher frequency of chromosome misalignment.

3.3.3 Soluble non-phosphorylatable katanin p60 decreases microtubule polymer and leads to misaligned chromosomes

The wildtype (WT) human katanin p60 tested above had a possible phosphorylation site at the exact same location in its sequence as *Xenopus laevis* katanin, serine 131 (predicted using GPS 3.0; www.gps.biocuckoo.org). A previous study on *Xenopus laevis* katanin p60 showed a serine site in the microtubule-binding domain (S131), when phosphorylated by Aurora B kinase, reduced the katanin p60 activity (Loughlin et al., 2011). Phosphorylation of

katanin p60 resulted in larger spindles in the frog oocyte and reduced severing *in vitro* (Loughlin et al., 2011; Whitehead et al., 2013). Overexpression of soluble p60 S131A also yielded a significant decrease in microtubule polymer (Figure 5). I found that WT katanin p60 expressed globally within mitotic cells caused misaligned chromosomes, but not major morphological phenotypes. Because human katanin p60 could also be inhibited by phosphorylation in the S2 cells, I globally expressed a mutant version of human katanin p60 replacing the serine at position 131 with an alanine (S131A, Figure 6B). I used transient overexpression of human katanin p60 S131A in S2 cells expressing GFP tubulin, and saw the same and examined the changes in mitosis (Figure 12A-D). I did not observe gross morphological changes, spindle length changes, or major changes in spindle dynamics in these cells. As with the WT katanin p60, there was an increase in misaligned chromosomes. I quantified the chromosomal misalignment for cells expressing soluble S131A katanin p60 mutant, relative to the internal control of non-expressing cells (Figure 12E). I found that the percentage of cells displaying misaligned chromosomes was 14 ± 2% for expressing cells compared to 5 ± 1% for non-expressing control cells in the same chamber (Figure 12E). The fold increase was 2.8 ± 0.7, which is significantly more than 1-fold, implying that this effect is truly caused by the katanin p60 expression (Figure 12F). The increase of chromosomal misalignment for katanin p60 S131A (2.8 ± 0.7) was within the uncertainty for the change for cells expressing katanin p60 WT (3.5 ± 0.9) (Figure 11F, Figure 12F). Thus, soluble

katanin p60 S131A led to the same level of misaligned chromosomes in mitosis as WT soluble katanin p60.

We did not observe gross morphological changes, spindle length changes, or major changes in spindle dynamics in these cells. As with the WT katanin p60, there was an increase in misaligned chromosomes. We quantified the chromosomal misalignment in cells expressing soluble S131A katanin p60 mutant, relative to the internal control of non-expressing cells (Figure 12E). I found that the percentage of cells displaying misaligned chromosomes was 14 ± 2% for expressing cells compared to 5 ± 1% for non-expressing control cells in the same chamber (Figure 12E). The fold increase was 2.8 ± 0.7, which is significantly more than 1-fold, implying that this effect is truly caused by the katanin p60 expression (Figure 12F). The increase of chromosomal misalignment for katanin p60 S131A (2.8 ± 0.7) was within the uncertainty for the change for cells expressing katanin p60 WT (3.5 ± 0.9) (Figure 11F and Figure 12F). Thus, soluble katanin p60 S131A led to the same level of misaligned chromosomes in mitosis as WT soluble katanin p60.

3.4 Conclusions

The tagged and untagged versions of human katanin p60 both show a decrease in microtubule polymer. Overexpression of soluble human katanin p60 WT or S131A led to no changes in spindle length or dynamics. An increase in cells with misaligned chromosomes were seen for both constructs. The increase of chromosomal misalignment for katanin p60 S131A (2.8 ± 0.7) was within the

uncertainty for the change for cells expressing katanin p60 WT (3.5 ± 0.9) (Figure 11F and Figure 12F). Thus, soluble S131A katanin p60 led to the same level of misaligned chromosomes in mitosis as soluble WT katanin p60. The presence of additional, active katanin p60 does not appear to be affecting spindle length in S2 cells.

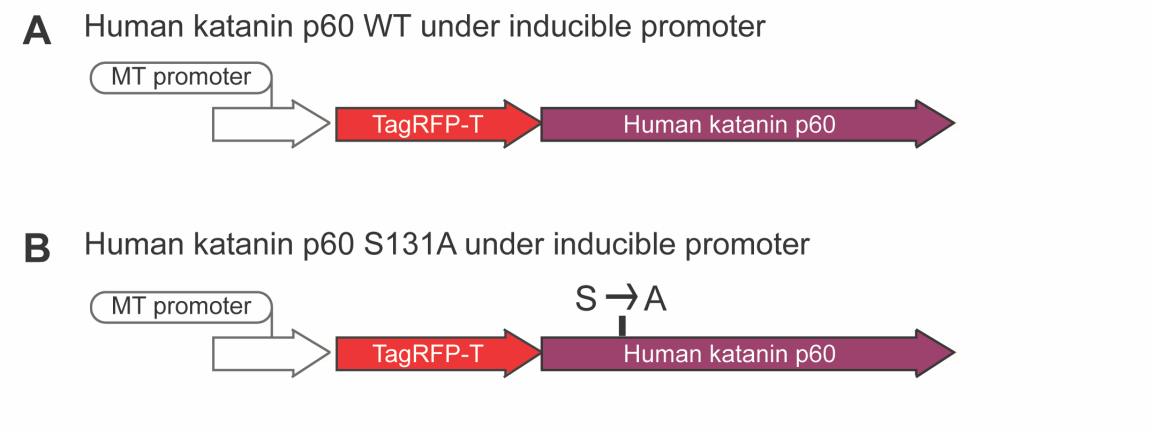

Figure 6: Constructs used in this study.
Constructs used in this study to create a microtubule disruption tool based on katanin p60. Each construct was made in pMT/V5-HisB plasmid with a Metallothionein (MT) promoter. **(A)** Human katanin p60 with TagRFP-T on the amino terminal end for global protein expression. **(B)** Human katanin p60 with serine to alanine mutation at amino acid 131 and TagRFP-T on the amino terminal end for global protein expression.

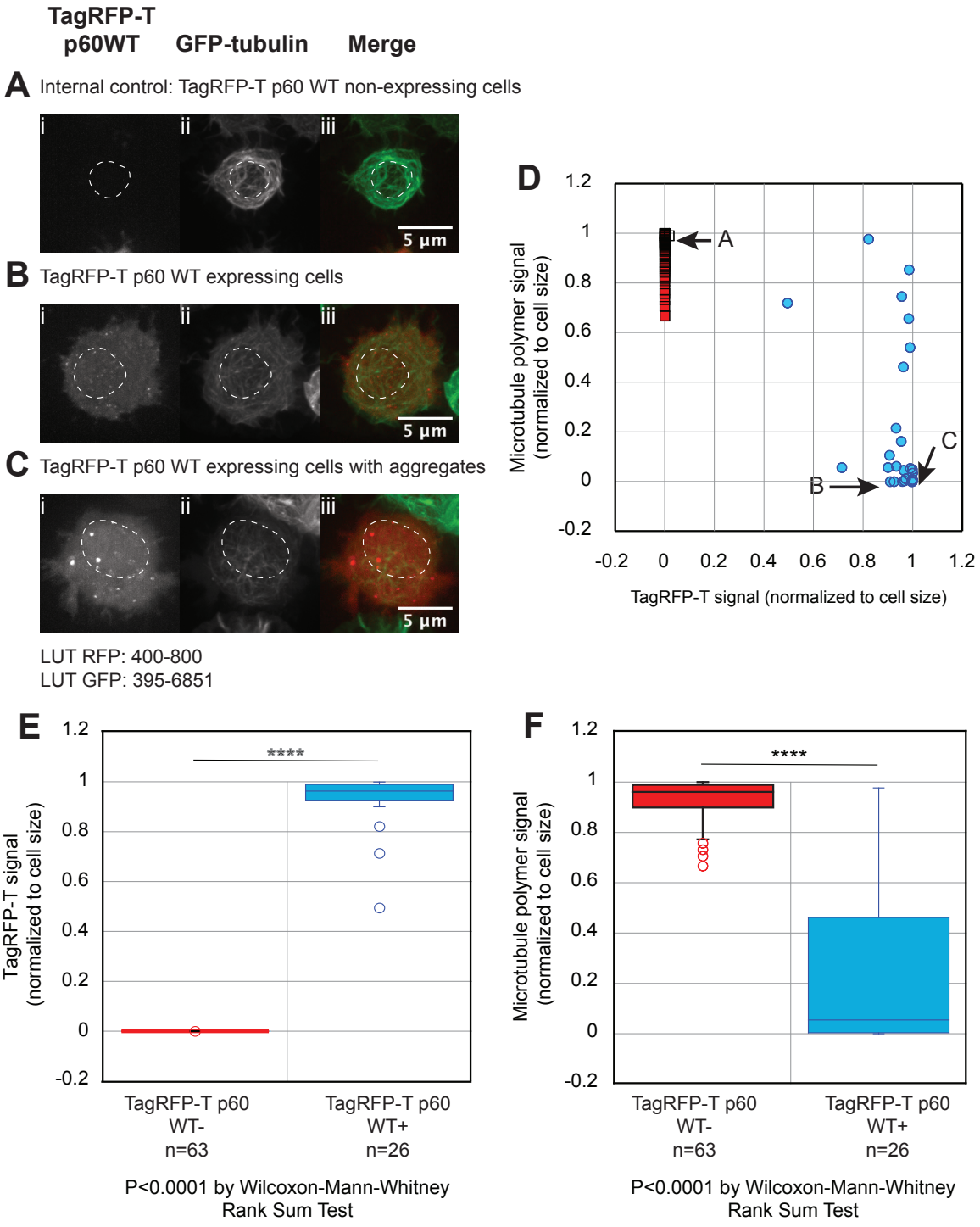

Figure 7: Quantification of TagRFP-T katanin p60 WT expression and microtubule polymer mass.

Live S2 cells transiently transfected with human katanin p60 WT were imaged to examine the GFP-microtubule polymer. (A) Example maximum projection of z-stack images with low expression of katanin showing (i) TagRFP-T katanin p60

WT signal with look up table (LUT) 400-800, (ii) GFP-tubulin signal with 395-6851 LUT settings. (iii) merged image of katanin (red) and microtubules (green). Position of the nucleus is shown using a dashed outline. (B) Example maximum projection of z-stack images with moderate expression of katanin showing (i) TagRFP-T katanin p60 WT signal with LUT 400-800, (ii) GFP-tubulin signal with 395-6851 LUT settings, (iii) merged image of katanin (red) and microtubules (green). Position of the nucleus is shown using a dashed outline. (C) Example maximum projection of z-stack images with high expression of katanin showing (i) TagRFP-T katanin p60 WT signal with look up table (LUT) 400-800 and demonstrating the tendency for katanin to aggregate at high expression, (ii) GFP-tubulin signal with 395-6851 LUT settings, (iii) merged image of katanin (red) and microtubules (green). Position of the nucleus is shown using a dashed outline. (D) Scatter plot of normalized GFP-microtubule signal (y-axis) as a function of normalized TagRFP-T katanin p60 expression signal (x-axis). Cells in the chamber that were not expressing katanin (red squares) are on the left side (N = 63 cells in 1 experiments). Cells in the chamber that were expressing katanin (blue circles) are on the right side (N = 26 cells in 1 experiment). (E) Box-whisker plot of quantification of TagRFP-T katanin signal (x-axis values from part D) in the non-expressing cells (red box) and expressing cells (blue box). The difference between the expressing and non-expressing intensities are significant ($P < 0.0001$). (F) Box-whisker plot of quantification of GFP-microtubule signal (y-axis values from part D) in the non-expressing cells (red box) and expressing cells (blue box). The difference between the expressing and non-expressing intensities are significant ($P < 0.0001$).

Z-stack through merged images of GFP-tubulin and TagRFP-T p60 WT

A Internal control: TagRFP-T p60WT non-expressing cells

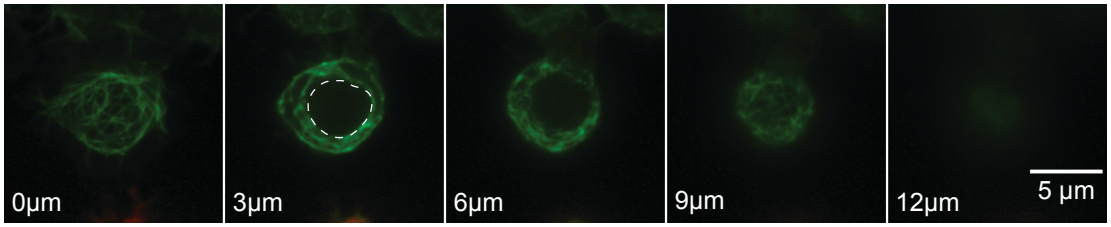

B TagRFP-T p60WT expressing cells showing decrease in MT polymer

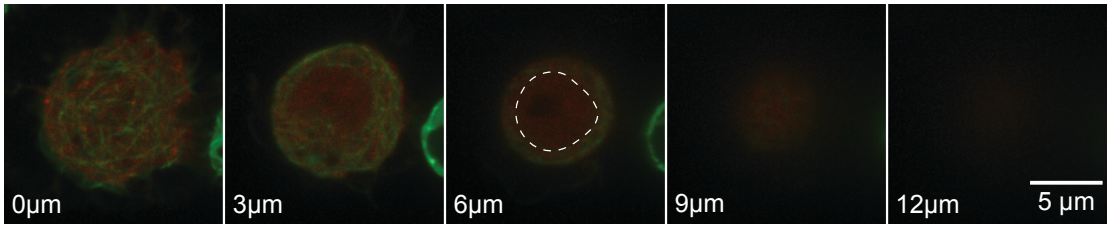

C TagRFP-T p60WT expressing cells showing some aggregates and a decrease in MT polymer

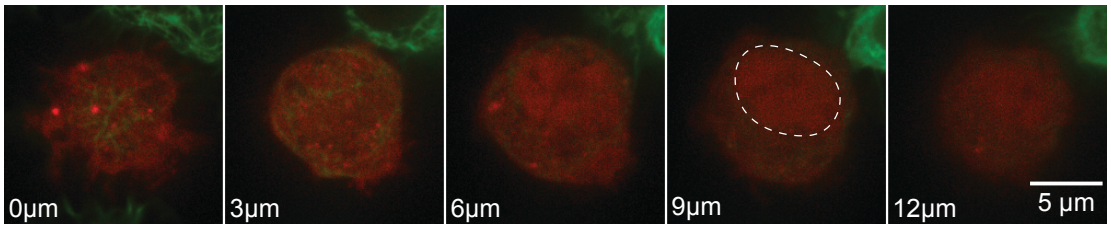

LUT RFP: 400-800
LUT GFP: 395-6851

Figure 8: Z-stack examples from soluble TagRFP-T katanin p60 WT expression.

For cells displayed as a maximum projection in figure 2, the location of the nucleus was determined using a z-stack through each cell. (A) Example z-stack of cell with low expression of katanin showing katanin (red) and microtubules (green) for heights from the bottom (0 µm) to the top (12 µm). Position of the nucleus is shown using a dashed outline. (B) Example z-stack of cell with moderate expression of katanin showing katanin (red) and microtubules (green) for heights from the bottom (0 µm) to the top (12 µm). Position of the nucleus is shown using a dashed outline. (C) Example z-stack of cell with high expression of katanin showing katanin (red) and microtubules (green) for heights from the bottom (0 µm) to the top (12 µm). Position of the nucleus is shown using a dashed outline. All scale bars represent 5 µm. The look up tables for RFP (400-800) and GFP (395-6851) are the same for all images.

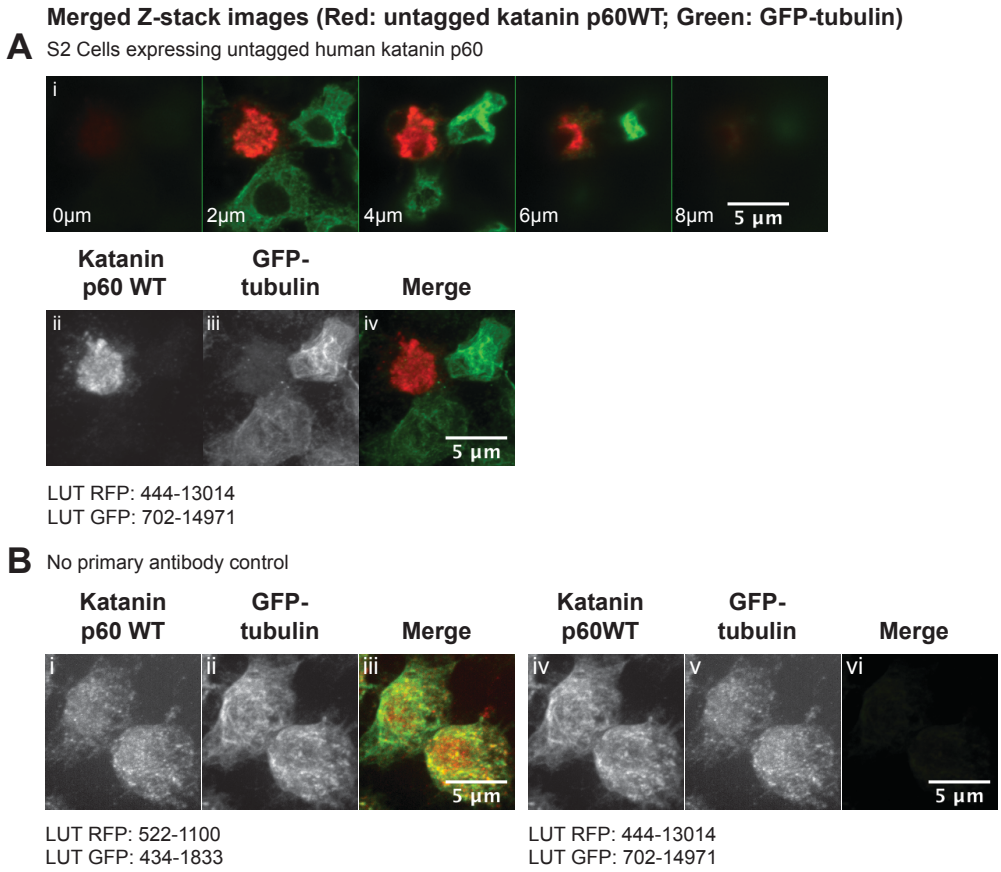

Figure 9: Immunofluorescence of global expression of wild type katanin p60 without TagRFP-T label.

Fixed S2 cells transiently transfected with katanin p60 without TagRFP-T. **(A)** Cells were stained with anti-tubulin (DM1α, green channel) and anti-human katanin p60 antibody 4F11 (red channel) and (i) imaged as z-stacks in spinning disc confocal microscopy, as described in the methods. Maximum projections of the (ii) katanin (red) and (iii) tubulin (green) channels were (iv) merged to show that some cells expressed katanin and had little to no microtubule staining. The look up tables displayed are 444-13014 for the red channel and 702-14971 for the green channel. **(B)** Using the same cells, I performed a control to stain with secondary antibodies without the primary staining to the (i) katanin antibody (red) and the (ii) tubulin antibody (green), (iii) merged. A look up table of 522-1100 for the red channel and 434-1833 for the green channel reveal global staining that might indicate katanin expression while maintaining high microtubule polymer mass. I find that the look up table choice can reveal background “noise” staining of the antibodies. If I use the same look up table as used in part (A), I find a slight staining in the (i) katanin antibody channel (red) and the (ii) tubulin antibody channel (green), (iii) merged, which could be mistaken for signal if the “optimal” look up table is used for this image.

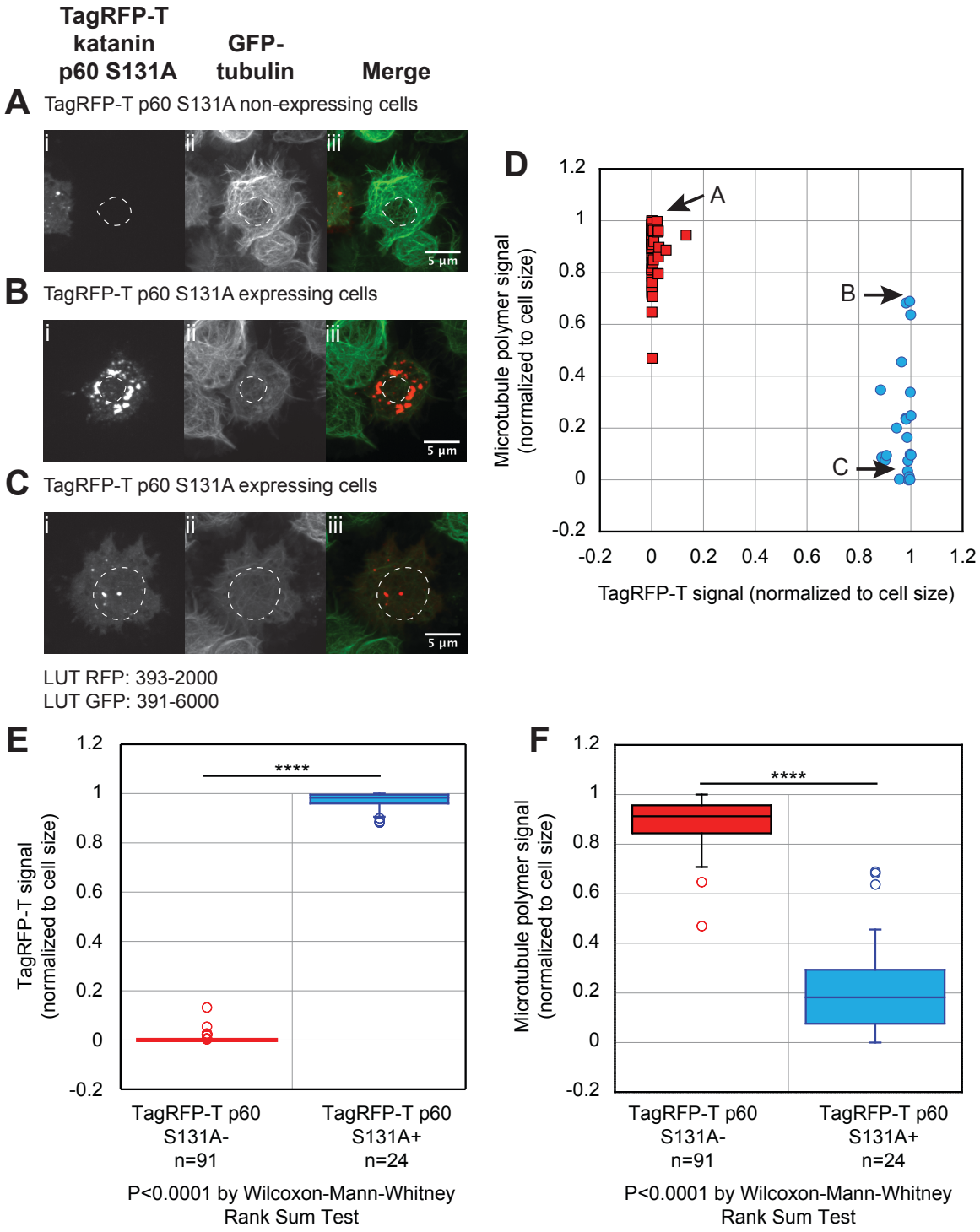

Figure 10: Quantification of TagRFP-T katanin p60 S131A expression and microtubule polymer mass.

Live S2 cells transiently transfected with human katanin p60 S131A were imaged to examine the GFP-microtubule polymer. (A) Example maximum projection of z-stack images with low expression of katanin showing (i) TagRFP-T katanin p60 S131A signal with LUT 393-2000, (ii) GFP-tubulin signal with 391-6000 LUT settings, and (iii) merged image of katanin (red) and microtubules (green).

Position of the nucleus is shown using a dashed outline. (B) Example maximum projection of z-stack images with moderate expression of katanin showing (i) TagRFP-T katanin p60 S131A signal with LUT 393-2000, (ii) GFP-tubulin signal with 391-6000 LUT settings, and (iii) merged image of katanin (red) and microtubules (green). Position of the nucleus is shown using a dashed outline. (C) Example maximum projection of z-stack images with high expression of katanin showing (i) TagRFP-T katanin p60 S131A signal with LUT 393-2000, (ii) GFP-tubulin signal with 391-6000 LUT settings, and (iii) merged image of katanin (red) and microtubules (green). Position of the nucleus is shown using a dashed outline. (D) Scatter plot of normalized GFP-microtubule signal (y-axis) as a function of normalized TagRFP-T katanin p60 expression signal (x-axis). Cells in the chamber that were not expressing katanin (red squares) are on the left side (N = 91 cells in 1 experiment). Cells in the chamber that were expressing katanin (blue circles) are on the right side (N = 24 cells in 1 experiment). (E) Box-whisker plot of quantification of TagRFP-T katanin signal (x-axis values from part D) in the non-expressing cells (red box) and expressing cells (blue box). The difference between the expressing and non-expressing intensities is significant ($P < 0.0001$). (F) Box-whisker plot of quantification of GFP-microtubule signal (y-axis values from part D) in the non-expressing cells (red box) and expressing cells (blue box). The difference between the expressing and non-expressing intensities is significant ($P < 0.0001$).

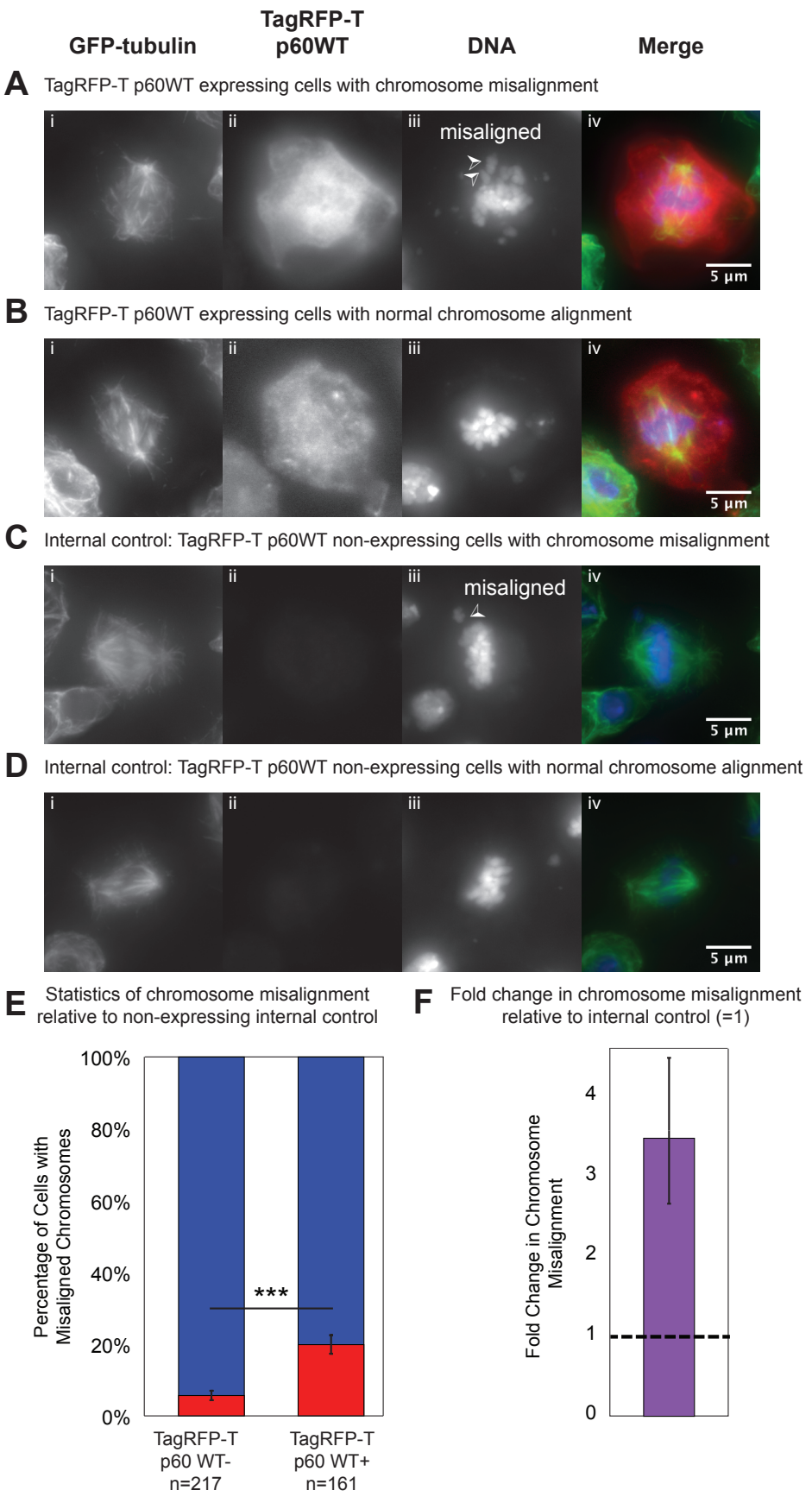
GFP-tubulin
TagRFP-T p60WT
DNA
Merge
A
TagRFP-T p60WT expressing cells with chromosome misalignment
i
ii
iii
misaligned
iv
5 µm
B
TagRFP-T p60WT expressing cells with normal chromosome alignment
i
ii
iii
iv
5 µm
C
Internal control: TagRFP-T p60WT non-expressing cells with chromosome misalignment
i
ii
iii
misaligned
iv
5 µm
D
Internal control: TagRFP-T p60WT non-expressing cells with normal chromosome alignment
i
ii
iii
iv
5 µm
E
Statistics of chromosome misalignment relative to non-expressing internal control
Percentage of Cells with Misaligned Chromosomes
100%
80%
60%
40%
20%
0%
***
TagRFP-T p60 WT- n=217
TagRFP-T p60 WT+ n=161
F
Fold change in chromosome misalignment relative to internal control (=1)
Fold Change in Chromosome Misalignment
4
3
2
1
0

Figure 11: Quantification of misaligned chromosome frequency with soluble WT katanin p60.

S2 cells transiently transfected with katanin p60 WT were arrested in metaphase, processed for immunofluorescence, and scored. Maximum projections of z-stack images of cells expressing katanin p60 WT with a **(A)** misaligned chromosome and **(B)** normal alignment. Non-expressing (internal control) cells with **(C)** misaligned chromosome and **(D)** normal alignment. For each panel **(A-D)**, I display **(i)** GFP-tubulin channel, **(ii)** TagRFP-T katanin p60 WT channel, **(iii)** DNA stained with DAPI, and **(iv)** merge of GFP-tubulin, TagRFP-T katanin, and DNA. Scale bars are 5 μm for all frames. **(E)** Quantification of the incidence of misaligned chromosomes (red bars) compared to normal alignment (blue bars) in cells expressing soluble p60 WT (N = 161 cells, 3 chambers) was greater than that for non-expressing cells (N = 217 cells, 3 chambers). The difference is significant because the $\chi 2 = 55.1$, with 1 degree of freedom (cut-off for significance at $P = 0.001$ was anything greater than 10.8). **(F)** Quantification of the fold change in misaligned chromosomes comparing expressing to non-expressing cells (purple bar). Error bars are accumulated measured uncertainty in the experiments. Dashed line indicates 1-fold change (no change).

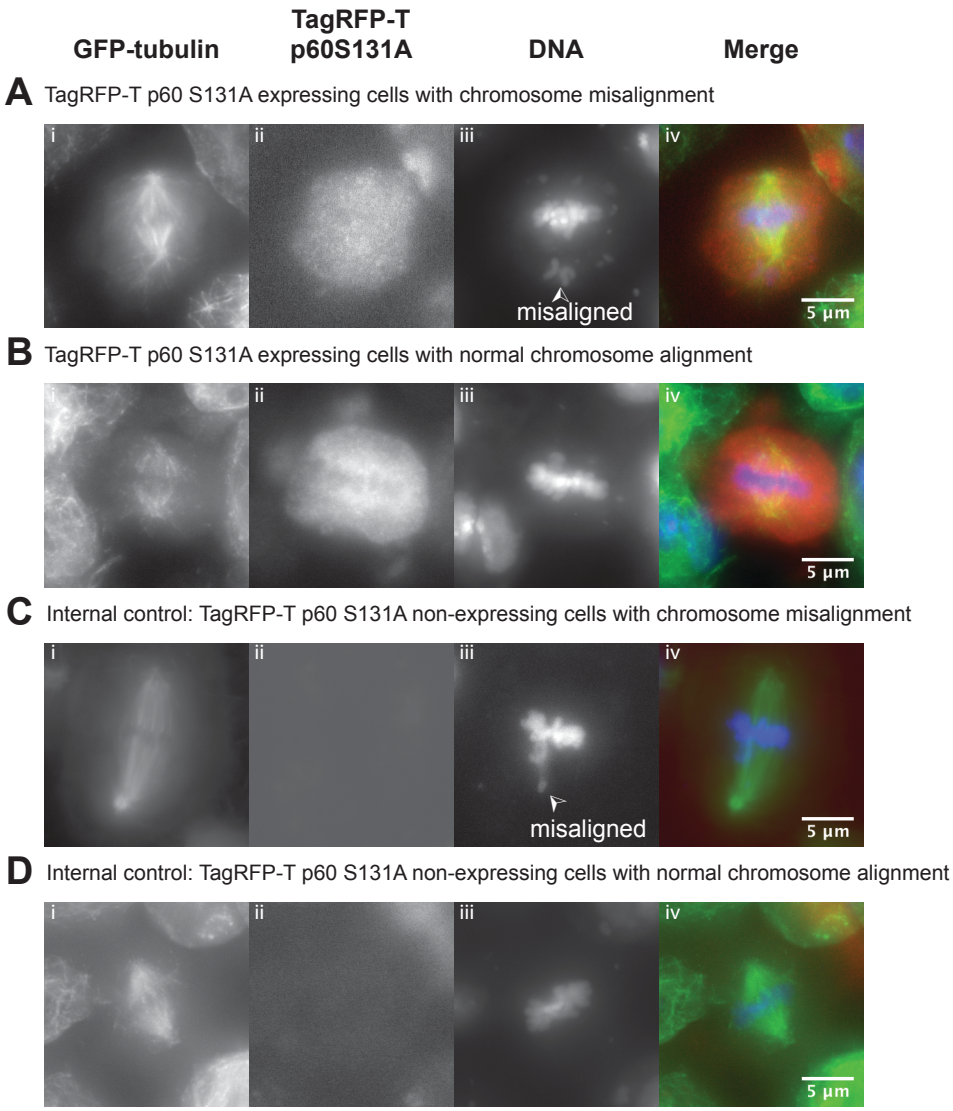
GFP-tubulin
TagRFP-T p60S131A
DNA
Merge
A TagRFP-T p60 S131A expressing cells with chromosome misalignment
i
ii
iii
iv
misaligned
5 µm
B TagRFP-T p60 S131A expressing cells with normal chromosome alignment
C Internal control: TagRFP-T p60 S131A non-expressing cells with chromosome misalignment
D Internal control: TagRFP-T p60 S131A non-expressing cells with normal chromosome alignment
E Statistics of chromosome misalignment relative to non-expressing internal control
Percentage of Cells with Misaligned Chromosomes
100%
80%
60%
40%
20%
0%
***
TagRFP-T p60 S131A- n=406
TagRFP-T p60 S131A+ n=281
F Fold change in chromosome misalignment relative to internal control (=1)
Fold Change in Chromosome Misalignment
4
3
2
1
0

Figure 12: Quantification of misaligned chromosome frequency with soluble katanin p60 S131A.

S2 cells transiently transfected with katanin p60 with serine to alanine mutation at amino acid 131 (S131A) were arrested in metaphase, processed for immunofluorescence, and scored. Maximum projections of z-stack images of cells expressing katanin p60 S131A with a **(A)** misaligned chromosome and **(B)** normal alignment. Non-expressing (internal control) cells with **(C)** misaligned chromosome and **(D)** normal alignment. For each panel **(A-D)**, I display **(i)** GFP-tubulin channel, **(ii)** TagRFP-T katanin p60 S131A channel, **(iii)** DNA stained with DAPI, and **(iv)** merge of GFP-tubulin, TagRFP-T katanin, and DNA. Scale bars are 5 μm for all frames. **(E)** Quantification of the incidence of misaligned chromosomes (red bars) compared to normal alignment (blue bars) in cells expressing soluble p60 WT (N = 281 cells, 3 chambers) was greater than that for non-expressing cells (N = 406 cells, 3 chambers). The difference is significant because the $\chi 2 = 30.5$, with 1 degree of freedom (cut-off for significance at $P = 0.001$ was anything greater than 10.8). **(F)** Quantification of the fold change in misaligned chromosomes comparing expressing to non-expressing cells (purple bar). Error bars are accumulated measured uncertainty in the experiments. Dashed line indicates 1-fold change (no change).

CHAPTER 4

TARGETED LOCALIZATION OF EXOGENOUS HUMAN KATANIN P60 WT AND S131A TO THE KINETOCHORE

4.1 Summary

In this chapter, I describe a new technique to localize human katanin p60 into living cells, using *Drosophila* S2 cells as the system. We chose the kinetochore as our target, expecting that an active katanin p60 at the kinetochore would be able to sever chromosome-k-fiber attachments and increase the frequency of misaligned chromosomes. This was not the case with the WT Mis12 p60 construct, as it gets inhibited by a high gradient of Aurora B kinase. Upon expression of a phosphomutant version of this construct, where the Aurora B phosphorylation at the serine 131 is replaced with alanine, we were able to obtain misaligned chromosomes.

4.2 Introduction

To disrupt cellular microtubules at a particular location and time, we are currently limited by low-throughput qualitative experiments using laser ablation. Laser ablation must be finely controlled, and tuned as to not damage other cellular structures and processes. It is also limited to a subset of cell types as laser power decreases to the sixth power of distance, so deeper regions of the cell cannot be accessed. Pharmacological methods, while high throughput, lack spatial resolution.

One issue with using a microtubule-severing enzyme as a microtubule-disruption agent is the global loss of polymer when it is ubiquitously

overexpressed (Figure 7 and Figure 10). However, high concentrations of katanin p60 are needed for microtubule depolymerization, because katanin p60 is a hexamer, and is inhibited by equimolar concentrations of free tubulin. These factors were considered in the final design scheme for the construct (**Error! Reference source not found.** and Figure 13). I chose to localize human katanin p60 to the kinetochore in S2 cells, with the expectation that high local concentrations would be obtained at this region, if tethered to a stable kinetochore protein such as Mis12 or Nuf2. The kinetochore can associate with microtubules via linkage to the KNL1-Mis12-Ndc80 network. Mis12 is a tetrameric protein and undergoes slow turnover when measured by FRAP (Hemmerich et al., 2008; Hori et al., 2003). We chose Mis12 for the following reasons: it is in greater proximity to the microtubules; is constitutively localized to centromeres in flies from as early as interphase (Venkei et al., 2012); and overexpressed Mis12 katanin p60 should be localized to the nucleus during interphase. Further, protein fusions with Mis12 are well-tolerated, as reported by several groups (Ballister et al., 2014; Maldonado & Kapoor, 2011).

4.3 Results

4.3.1 Effects of Mis12 p60WT and S131A overexpression

To obtain an idea of relative expression levels for the two proteins, we chose to quantify their relative phenotypic effects compared to protein expression levels so that any change in microtubule polymer could be attributed changes in microtubule polymer. The protein expression levels of katanin p60 and Mis12 p60 were quite different. First, I noticed that the area density of TagRFP-T Mis12

katanin p60 was significantly reduced compared to the previously observed global expression of TagRFP-T katanin p60, with intensities about half that of the global expression (Figure 7D, Figure 14C). Representing the TagRFP-T Mis12 katanin p60 density signal data as a box-whisker plot to show that there is still a significant increase in the TagRFP-T signal compared to non-expressing control cells in the same chamber (Figure 14D, $P < 0.0001$).

When comparing the TagRFP-T densities between global expression and Mis12 linkage, the tethering of katanin p60 to Mis12 causes a significant loss of TagRFP-T density ($P < 0.0001$ KS Test, Figure 7E compared to Figure 14E, blue bars). Close inspection shows that the TagRFP-T Mis12 katanin p60 was aggregated in cells in both the cell body and nucleus (Figure 14, B). Unlike for TagRFP-T katanin p60, the addition of the Mis12 exacerbated aggregation such that there was barely detectable soluble pool of TagRFP-T Mis12 katanin p60.

Stable cell lines expressing Mis12p60 WT or Mis12p60 S131A were induced overnight for expression, as described in the Methods. The next day, a small sample of cells were allowed to spread on ConA-coated dishes and coverslips so that they could be quantified for microtubule polymer or misaligned chromosomes.

We observed no change in gross phenotypes, such as spindle length, and positioning, in cells expressing Mis12 p60 WT or S131A during metaphase. When comparing the TagRFP-T densities between global expression and Mis12 linkage, the Mis12 causes a significant loss of density ($P < 0.0001$ KS Test,

Figure 7E compared to Figure 14D, blue bars). Close inspection shows that the TagRFP-T Mis12 katanin p60 was aggregated in cells in both the cell body and nucleus (Figure 14A, B). Unlike for TagRFP-T katanin p60, the addition of the Mis12 exacerbated aggregation such that there was barely detectable soluble pool of TagRFP-T Mis12 katanin p60. We suspect that katanin p60 in aggregates is not functional *in vivo*, and only the soluble pool is capable of destroying microtubule polymer in cells. This is based on our prior *in vitro* studies on katanin p60 activity, where highly concentrated preparations of katanin were observed to be inactive and had significant aggregation (unpublished data). We have since moved to a Maltose-Binding Protein affinity purification system that significantly reduces aggregation of purified proteins and enhances the activity of the purified katanin (Loughlin et al., 2011). Our results suggest that katanin aggregates observed in cells occur as a consequence of high concentration of katanin and is increased due to the tethering to Mis12. In cells that only have aggregates, the microtubules remain without observable loss of polymer. In cells with a significant soluble pool of TagRFP-T katanin p60 in addition to aggregates, the microtubule polymer mass is significantly reduced (comparing Figure 14A,B to Figure 7B,C).

4.3.2 Quantification of TagRFP-T signal in cells expressing soluble katanin p60 and Mis12 p60

We needed to demonstrate that the overexpression of katanin p60 fused to Mis12 would not globally disrupt interphase microtubules. We used stable S2 cell lines that expressed TagRFP-T Mis12 katanin p60 when induced by copper

sulfate, and proceeded to quantify microtubule polymer in live S2 cells, as described in the Methods.

We observed no change in gross phenotypes, such as spindle length, and positioning, in cells expressing Mis12p60 WT or S131A during metaphase. When comparing the TagRFP-T densities between global expression and Mis12 linkage, the Mis12 causes a significant loss of density ($P < 0.0001$ KS Test, Figure 7E compared to Figure 14D, blue bars). Close inspection shows that the TagRFP-T Mis12 katanin p60 was aggregated in cells in both the cell body and nucleus (Figure 14A,B and Figure 17A,B). Unlike for TagRFP-T katanin p60 to Figure 7B,C), the addition of the Mis12 exacerbated aggregation such that there was barely detectable soluble pool of TagRFP-T Mis12 katanin p60. We suspect that katanin p60 in aggregates is not functional *in vivo*, and only the soluble pool is capable of destroying microtubule polymer in cells. This is based on our prior *in vitro* studies on katanin p60 activity, where highly concentrated preparations of katanin were observed to be inactive and had significant aggregation (unpublished data). We have since moved to a Maltose-Binding Protein affinity purification system that significantly reduces aggregation of purified proteins and enhances the activity of the purified katanin (Loughlin et al., 2011). Our results suggest that katanin aggregates observed in cells occur as a consequence of high concentration of katanin and is increased due to the tethering to Mis12. In cells that only have aggregates, the microtubules remain without observable loss of polymer. In cells with a significant soluble pool of TagRFP-T katanin p60 in

addition to aggregates, the microtubule polymer mass is significantly reduced (comparing Figure 14A,B and Figure 17A,B to Figure 7B,C).

4.3.3 Quantification of microtubule polymer in Mis12p60WT and Mis12p60S131A cells

We needed to demonstrate that the overexpression of katanin p60 fused to Mis12 would not globally disrupt interphase microtubules. We used stable S2 cell lines that expressed TagRFP-T Mis12 katanin p60 when induced by copper sulfate, as described in the Methods.

We quantified the microtubule network signal data and represented it as a box-whisker plot to highlight that we observed no significant difference in the microtubule polymer between TagRFP-T Mis12 katanin p60 WT expressing and non-expressing cells (Figure 14E, $P = 0.48$ using the Wilcoxon-Mann-Whitney test). We also used the K-S Test and found the relative area fraction for expressing cells (median = 0.88, standard deviation = 0.14, N=143) and non-expressing cells (median = 0.90, standard deviation = 0.11, N=185), were statistically indistinguishable ($P = 0.096$). This is not surprising given that the TagRFP-T Mis12 katanin p60 WT was all aggregated in these cells with no soluble katanin pool. We had hoped that the Mis12 would localize the TagRFP-T Mis12 katanin p60 WT to the nucleus to inactivate it during interphase. Instead, Mis12 helped to aggregate the katanin p60, which may have sequestered and inactivated its microtubule-destruction abilities. Despite not working as we expected, the result is as desired for a targeted microtubule-disruption tool.

As with global expression of TagRFP-T katanin p60 WT, we imaged and quantified the GFP-microtubule polymer and TagRFP-T Mis12 katanin p60 signal (Figure 14A, B). The measured density of both the microtubule network and the TagRFP-T Mis12 katanin p60 were normalized by the size of the cell and plotted with TagRFP-T Mis12 katanin p60 signal on the x-axis and GFP-microtubule signal on the y-axis (Figure 14C).

4.3.4 Localization of Mis12-katanin p60 to the kinetochore

We have demonstrated above, that our microtubule-disruption tool, when localized to the Mis12 complex, does not globally disrupt the microtubule network in interphase. We next wanted to test if the TagRFP-T Mis12 katanin p60 WT construct is localized to the kinetochore in mitosis (Figure 13). We expected that fusing katanin p60 to Mis12 would localize to the kinetochore during mitosis. Using immunofluorescence staining with antibodies against TagRFP-T, GFP-tubulin, and human katanin p60, we observed both the N-terminal TagRFP-T and the C-terminal katanin p60 signals overlap at the kinetochore (Figure 15). This indicated that a full-length fusion protein was expressed and localized to the *Drosophila* kinetochore.

4.3.5 Mis12-katanin p60 activity at kinetochores during mitosis

After demonstrating the localization of human katanin p60 to the kinetochore via Mis12, we tested if human katanin p60 was active at the kinetochores. Active human katanin p60 at this position could have a variety of effects. We directly imaged stable S2 cells expressing inducible WT human katanin p60 fused to

Mis12 during mitosis (Figure 15A-D). We did not find any large changes to spindle architecture upon inspection.

Above, we found that soluble katanin p60 was able to induce a chromosomal misalignment phenotype. Since there were no gross morphological changes, it is possible that TagRFP-T Mis12 katanin p60 WT protein localized to the kinetochores could also cause a chromosomal misalignment. When we quantified the misalignment of chromosomes for cells expressing TagRFP-T Mis12 katanin p60 WT protein, we found no significant change in misaligned chromosomes, 7 ± 2%, compared to the non-expressing cells, 5 ± 1% (Figure 16). This change was a minor 1.4 ± 0.4-fold increase, indistinguishable from a 1-fold change (Figure 16F). We performed Chi-squared statistical analysis ($\chi 2$ = 0.557, degrees of freedom = 1) and found no difference between these results, as expected, given the uncertainty values we measured. We concluded that the WT katanin p60 placed at the kinetochore via Mis12 does not cause a chromosome misalignment phenotype.

The lack of an effect on chromosome alignment or spindle morphology with the TagRFP-T Mis12 katanin p60 WT construct was most likely due to local inhibition of human katanin p60 by Aurora B kinase emanating from centromeres (Figure 16). As described above, the S131 site is a target for Aurora B kinase in *Xenopus laevis* p60, but is absent in *Xenopus tropicalis* (Loughlin et al., 2011). To determine if our katanin p60 tool was affected by Aurora B kinase, we created a point mutation where serine at amino acid 131 was mutated to alanine (S131A)

(Figure 13). Since this construct could not be phosphorylated at that amino acid residue, the TagRFP-T Mis12 katanin p60 S131A should retain activity at kinetochores.

To test if human katanin p60 localized to the kinetochores is being turned off by Aurora B kinase, we produced a stable cell line expressing an inducible TagRFP-T Mis12 katanin p60 S131A. We first quantified the microtubule density as a function of TagRFP-T density in cells during interphase (Figure 17). We found that the expression levels, aggregation, and inability to destroy microtubules globally during interphase was identical for the S131A version as it was for the wild type version of TagRFP-T Mis12 katanin p60 (Figure 17).

Next, we tested the ability of TagRFP-T Mis12 katanin p60 S131A to alter chromosome alignment using widefield microscopy (Figure 18A-D). We observed a significant increase in cells with misaligned chromosomes for the Mis12 katanin p60 S131A-expressing cells, 22 ± 4%, relative to the internal control of non-expressing cells in the same chamber, 10 ± 3% (Figure 18E). The katanin p60 S131A localized to the kinetochores caused a 2.3 ± 0.7-fold increase in chromosomal misalignment, which is significantly different from a 1-fold change (Figure 18F). These results imply that the human katanin p60 can be inhibited by Aurora B kinase-mediated phosphorylation at S131, and that phosphorylation significantly reduces the activity of the kinetochore-targeted human katanin p60 in S2 cells. Further, the fact that TagRFP-T Mis12 katanin p60 WT did not result in an increase in chromosome misalignment means that the katanin p60 is

effectively targeted to the kinetochore and turned off, since global expression of the WT katanin p60 resulted in chromosome misalignment. Our results imply that we have successfully created and targeted a microtubule-disrupting tool to the kinetochore.

4.4 Conclusions

We suspect that katanin p60 in aggregates is not functional in vivo, and only the soluble pool is capable of destroying microtubule polymer in cells. This is based on our prior in vitro studies on katanin p60 activity, where highly concentrated preparations of katanin were observed to be inactive and had significant aggregation (unpublished data). We have since moved to a Maltose-Binding Protein affinity purification system that significantly reduces aggregation of purified proteins and enhances the activity of the purified katanin (Loughlin et al., 2011). Our results suggest that katanin aggregates observed in cells occur as a consequence of high concentration of katanin and is increased due to the tethering to Mis12. In cells that only have aggregates, the microtubules remain without observable loss of polymer. In cells with a significant soluble pool of TagRFP-T katanin p60 in addition to aggregates, the microtubule polymer mass is significantly reduced (comparing Figure 14A,B to Figure 7B,C).

Overall, these results inform us that our TagRFP-T Mis12 katanin p60 microtubule disruption tool does the following. First, the human katanin p60 construct was active in S2 cells and could remove fly microtubules (Figure 7, Figure 10). Second, the Mis12 fusion could inactivate katanin p60 in interphase

to keep the tool sequestered and away from interphase microtubules (Figure 14, Figure 17). In mitosis, the Mis12 fusion localized human katanin p60 to kinetochores (Figure 15).

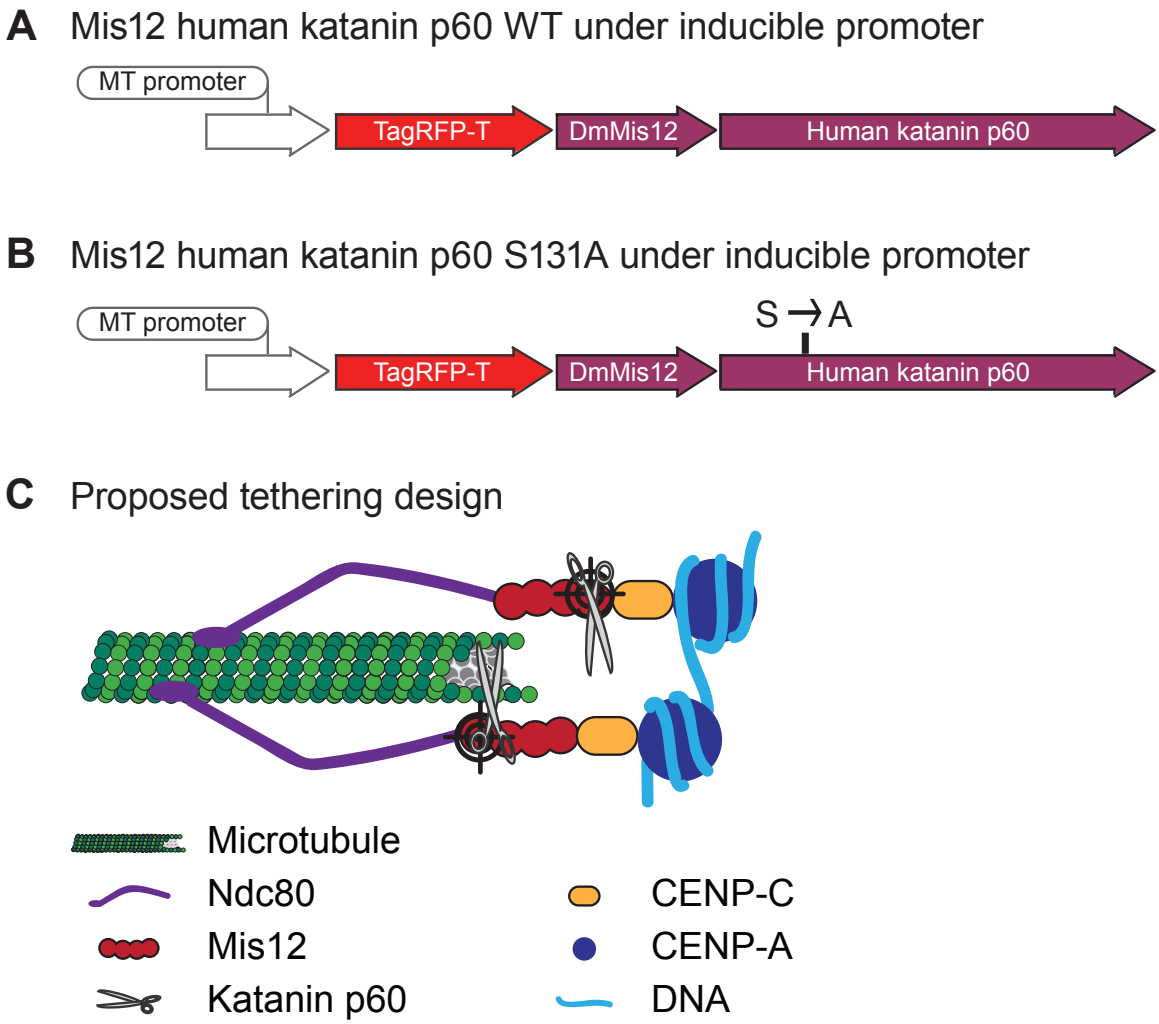

Figure 13: Constructs used in this study.

Constructs used in this study to create a microtubule disruption tool based on katanin p60. Each construct was made in pMT/V5-HisB plasmid with a Metallothionein (MT) promoter. (A) Chimera construct of Drosophila Mis12, TagRFP-T, and human katanin p60 for localization at kinetochores. (B) Chimera construct of Drosophila Mis12, TagRFP-T, and human katanin p60 with serine to alanine mutation at amino acid 131 for localization at kinetochores. (C) Cartoon demonstrating the expected localization of chimeric constructs containing Drosophila Mis12 and human katanin p60 at the kinetochore of S2 cells.

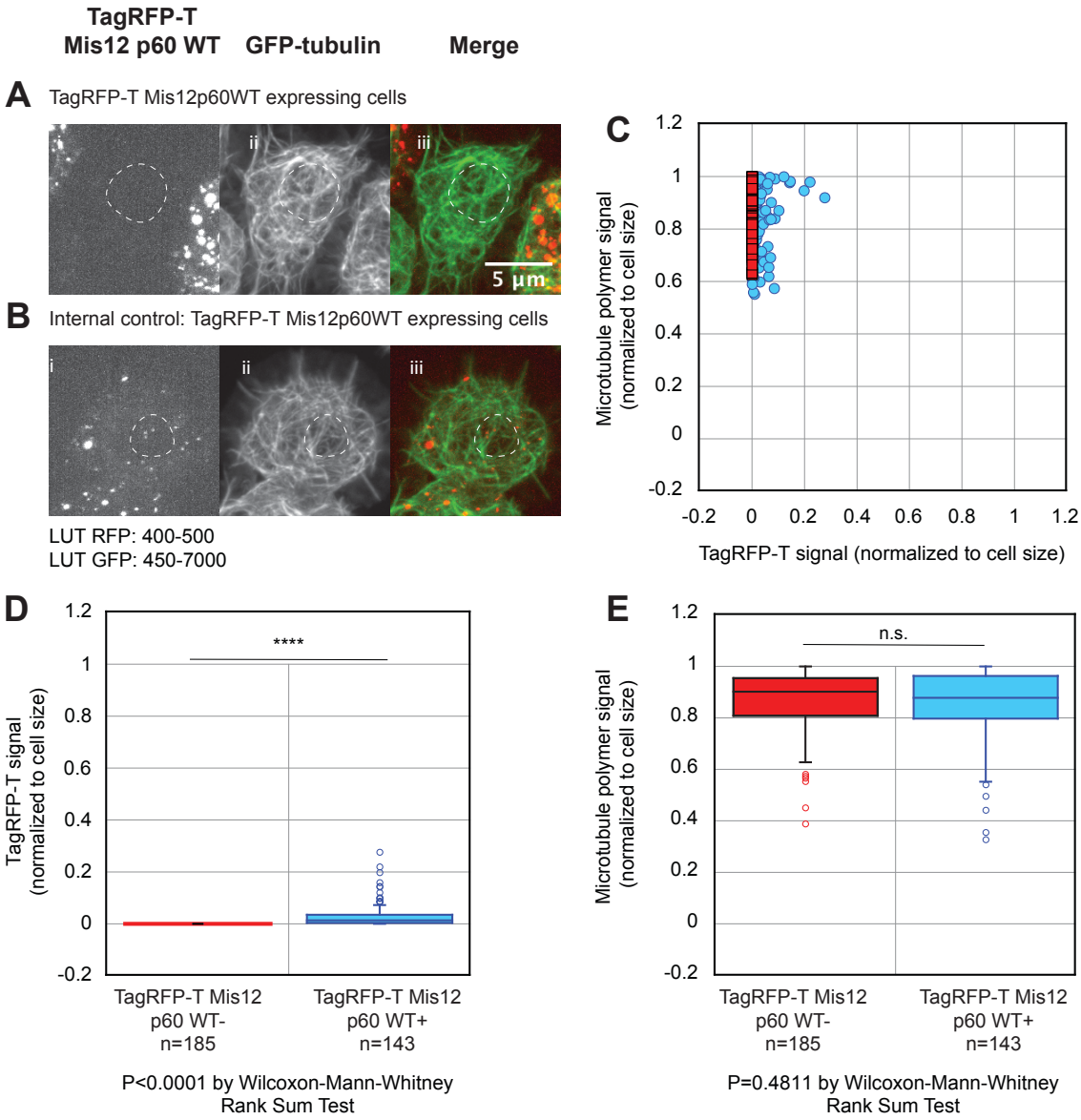

Figure 14: Quantification of TagRFP-T Mis12 katanin p60 WT and microtubule polymer mass in interphase.

Live S2 cells stably expressing Mis12 TagRFP-T human katanin p60 WT were imaged to examine the GFP-microtubule polymer. (A) Example maximum projection of z-stack images with low expression of katanin showing (i) Mis12 TagRFP-T katanin p60 signal with 400-500 LUT, (ii) GFP-tubulin signal with 450-7000 LUT settings, (iii) merged image of katanin (red) and microtubules (green). Position of the nucleus is shown using a dashed outline. (B) Example maximum projection of z-stack images with moderate expression of katanin showing (i) Mis12 TagRFP-T katanin p60 WT signal with LUT 400-500, (ii) GFP-tubulin signal with 450-7000 LUT settings, (iii) merged image of katanin (red) and microtubules (green). Position of the nucleus is shown using a dashed outline. (C) Scatter plot of normalized GFP- microtubule signal (y-axis) as a function of normalized Mis12 TagRFP-T katanin p60 expression signal (x-axis). Cells in the

chamber that were not expressing katanin (red squares) are on the left side (N = 185 cells in 3 experiments) Cells in the chamber that were expressing katanin (blue circles) are on the right side (N = 143 cells in 3 experiment). (D) Box-whisker plot of quantification of TagRFP-T katanin signal (x-axis values from part C) in the non-expressing cells (red box) and expressing cells (blue box). The difference between the expressing and non-expressing intensities are significant ($P < 0.0001$). (E) Box- whisker plot of quantification of GFP-microtubule signal (y-axis values from part C) in the non- expressing cells (red box) and expressing cells (blue box). The difference between the expressing and non-expressing intensities is not significant ($P < 0.49$).

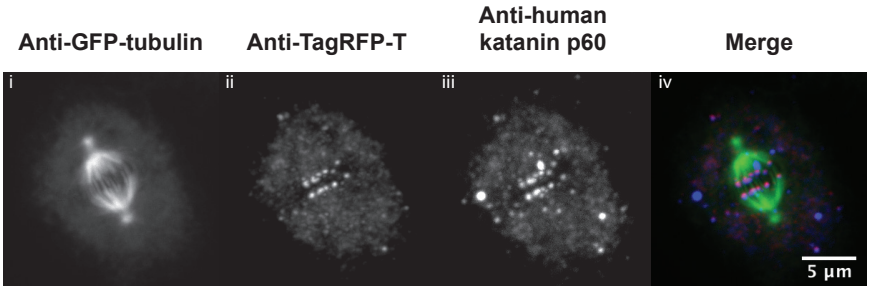

Figure 15: Kinetochore localization of TagRFP-T Mis12 katanin p60 WT in mitosis.

Immunofluorescence staining of fixed mitotic cell expressing TagRFP-T Mis12 katanin p60 shows localization of katanin to the kinetochores when stained for (i) GFP-tubulin, (ii) TagRFP-T, and (iii) human katanin p60. (iv) Merged images show overlap of the TagRFP and katanin signals with expected localization of kinetochore implying that the Mis12 is capable of localizing the katanin to the correct location during mitosis.

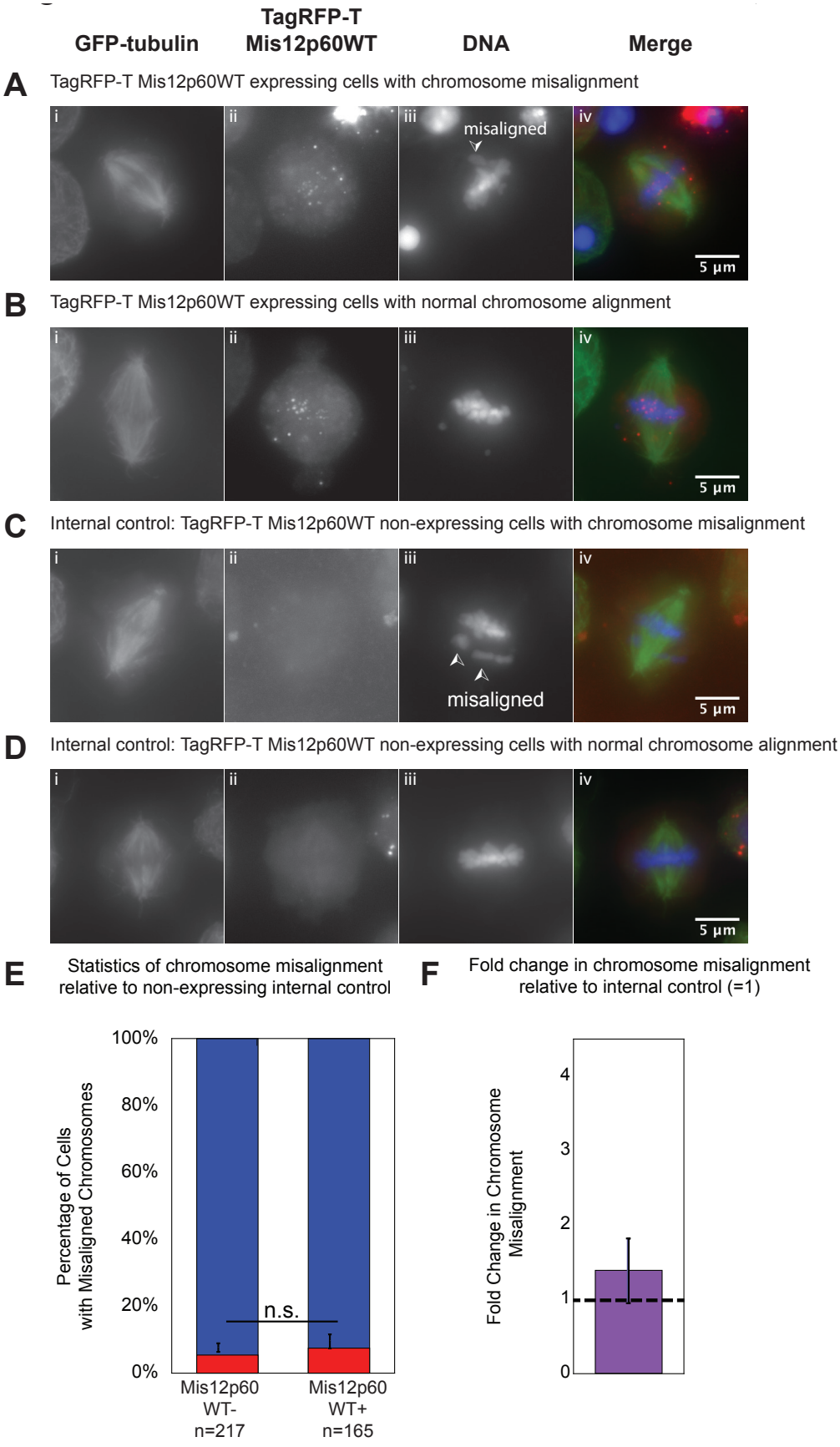
GFP-tubulin
TagRFP-T Mis12p60WT
DNA
Merge
A
TagRFP-T Mis12p60WT expressing cells with chromosome misalignment
misaligned
5 µm
B
TagRFP-T Mis12p60WT expressing cells with normal chromosome alignment
5 µm
C
Internal control: TagRFP-T Mis12p60WT non-expressing cells with chromosome misalignment
misaligned
5 µm
D
Internal control: TagRFP-T Mis12p60WT non-expressing cells with normal chromosome alignment
5 µm
E
Statistics of chromosome misalignment relative to non-expressing internal control
Percentage of Cells with Misaligned Chromosomes
100%
80%
60%
40%
20%
0%
n.s.
Mis12p60 WT- n=217
Mis12p60 WT+ n=165
F
Fold change in chromosome misalignment relative to internal control (=1)
Fold Change in Chromosome Misalignment
4
3
2
1
0

Figure 16: Quantification of misaligned chromosome frequency with Mis12 p60 WT.

S2 cells stably expressing TagRFP-T Mis12 WT katanin p60 were arrested in metaphase, processed for immunofluorescence, and scored. Maximum projections of z-stack images of cells expressing Mis12 katanin p60 with a (A) misaligned chromosome and (B) normal alignment. Non-expressing (internal control) cells with (C) misaligned chromosome and (D) normal alignment. For each panel (A-D), we display (i) GFP-tubulin channel, (ii) Mis12 TagRFP-T katanin p60 channel, (iii) DNA stained with DAPI, and (iv) merge of GFP-tubulin, Mis12 TagRFP-T katanin, and DNA. Scale bars are 5 μm for all frames. (E) Quantification of the incidence of misaligned chromosomes (red bars) compared to normal alignment (blue bars) in cells expressing Mis12 TagRFP-T katanin p60 (N = 217 cells, 3 chambers) was the same as that for non-expressing cells (N = 165 cells, 3 chambers). The difference is not significant because the $\chi 2 = 0.56$, with 1 degree of freedom (cut-off for significance at $P = 0.05$ was anything greater than 3.84). (F) Quantification of the fold change in misaligned chromosomes comparing expressing to non-expressing cells (purple bar). Error bars are accumulated measured uncertainty in the experiments. Dashed line indicates 1-fold change (no change).

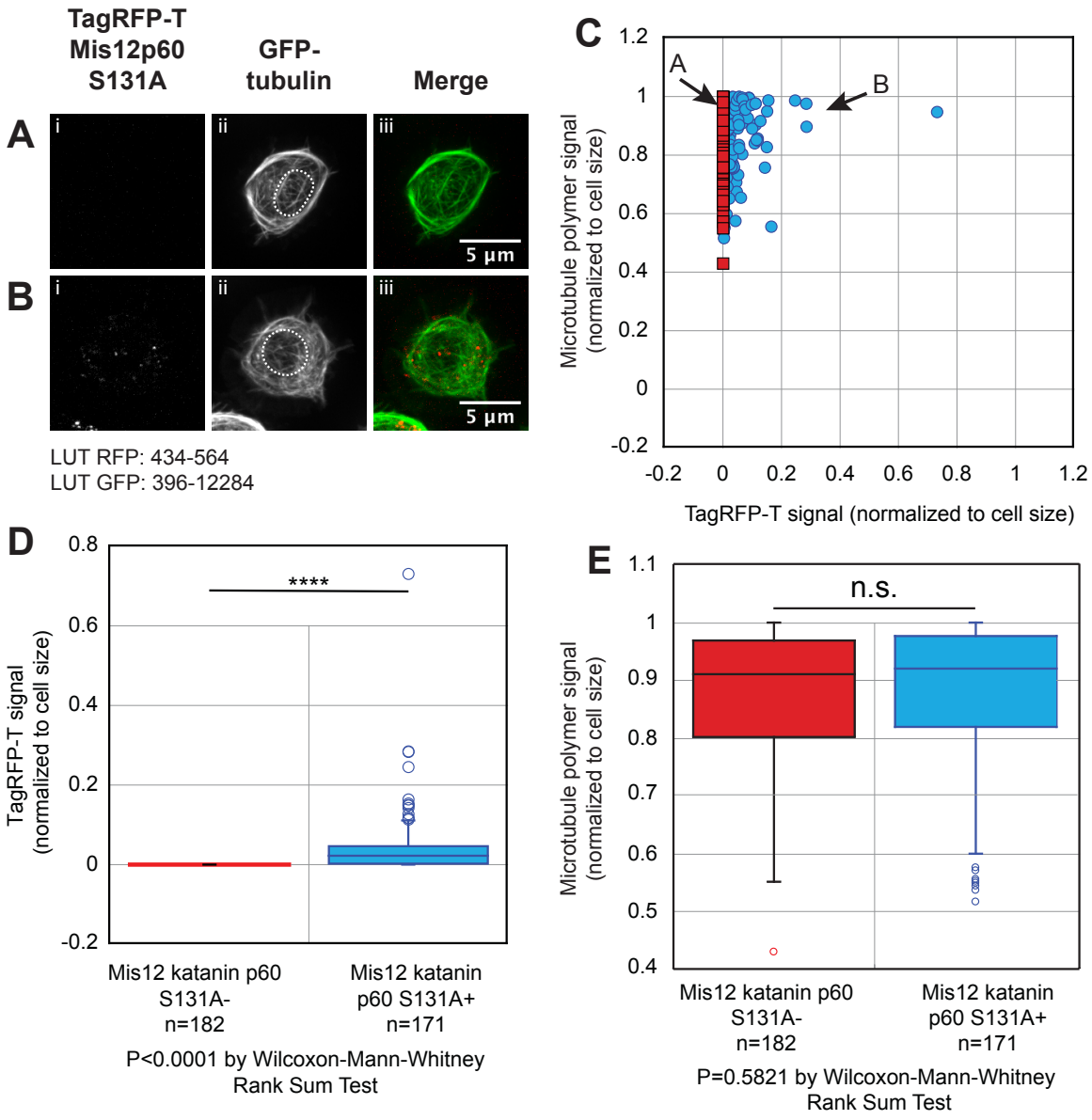

Figure 17: Quantification of tubulin for Mis12 katanin p60 S131A in interphase cells.

Live S2 cell lines stably expressing TagRFP-T Mis12 katanin p60 S131A were imaged to examine the GFP-microtubule polymer. (A)Example maximum projection of z-stack images with (1) high expression and (2) low expression of katanin showing (i)TagRFP-T katanin p60 S131A signal with LUT 432-564, (ii)GFP-tubulin signal with 396-12284 LUT settings, and (iii) merged image of katanin (red) and microtubules (green). Position of the nucleus is shown using a dashed outline. (B)Scatter plot of normalized GFP-microtubule signal (y-axis) as a function of normalized TagRFP-T katanin p60 expression signal (x-axis). Cells in the chamber that were not expressing katanin (red squares) are on the left side (N = 182 cells in 3 experiments). Cells in the chamber that were expressing katanin (blue circles) are toward the right side (N = 171 cells in 3 experiments). (C) Box-whisker plot of quantification of TagRFP-T katanin signal (x-axis values

from part B) in the non-expressing cells (red box) and expressing cells (blue box). The difference between the expressing and non-expressing intensities is significant ($P < 0.0001$). (D) Box-whisker plot of quantification of GFP-microtubule signal (y-axis values from part D) in the non-expressing cells (red box) and expressing cells (blue box). No significant difference between the expressing and non-expressing intensities was measured ($P = 0.58$).

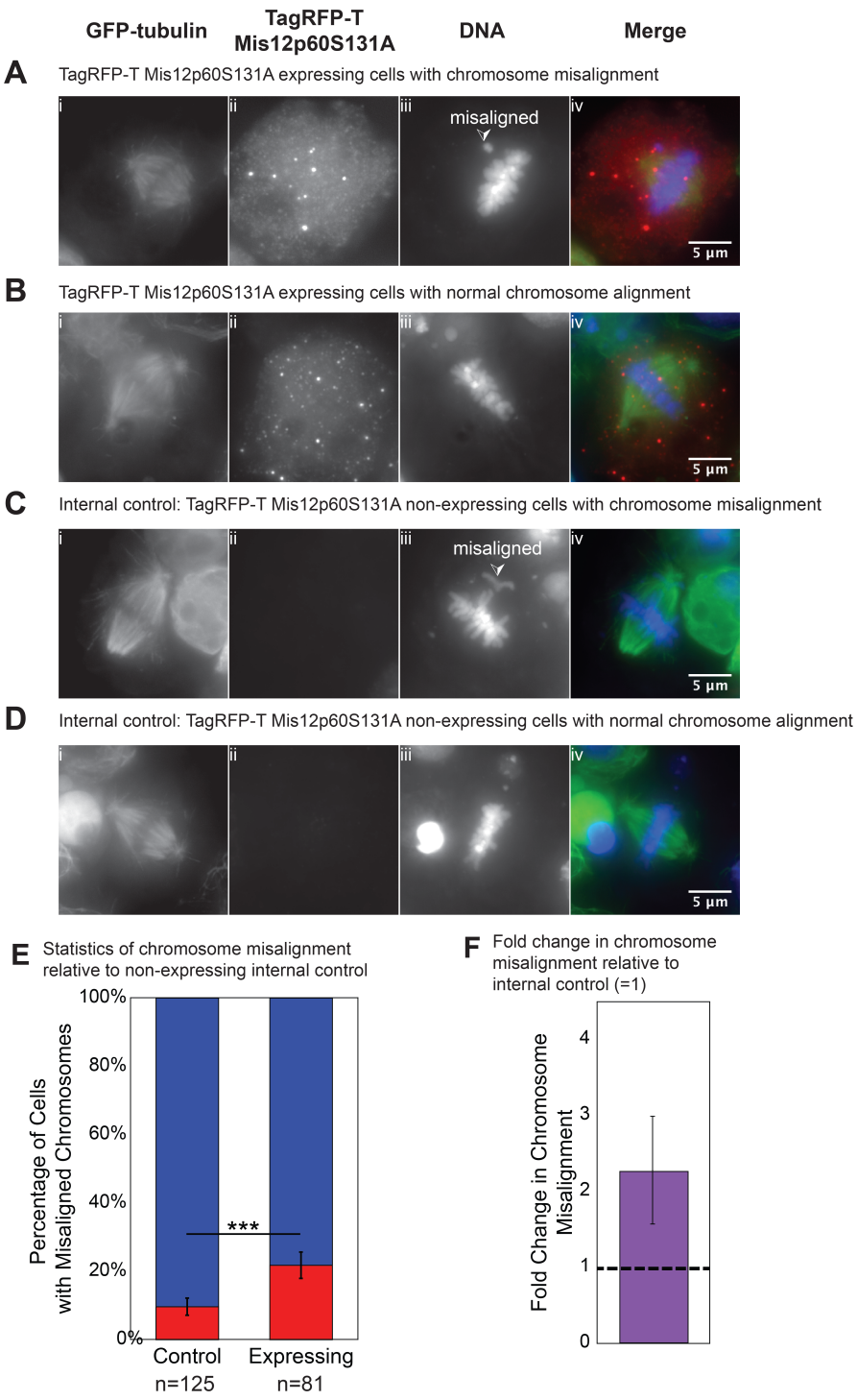

Figure 18: Quantification of misaligned chromosome frequency with Mis12-p60 S131A: A localized microtubule-disruption tool.

S2 cells stably expressing TagRFP-T Mis12 katanin p60 with an alanine to serine mutation at amino acid 131 (S131A) were arrested in metaphase, processed for immunofluorescence, and scored. Maximum projections of z-stack images of cells expressing Mis12 katanin p60 with a (A) misaligned chromosome and (B)

normal alignment. Non-expressing (internal control) cells with (C) misaligned chromosome and (D) normal alignment. For each panel (A-D), we display (i) GFP-tubulin channel, (ii) Mis12 TagRFP-T katanin p60 channel, (iii) DNA stained with DAPI, and (iv) merge of GFP-tubulin, Mis12 TagRFP-T katanin, and DNA. Scale bars are 5 μm for all frames. (E) Quantification of the incidence of misaligned chromosomes (red bars) compared to normal alignment (blue bars) in cells expressing Mis12 TagRFP-T p60 S131A (N = 122 cells, 3 chambers) was greater than that for non-expressing cells (N = 115 cells, 3 chambers). The difference is significant because the $\chi 2 = 19.8$, with 1 degree of freedom (cut-off for significance at $P = 0.001$ was anything greater than 10.8). (F) Quantification of the fold change in misaligned chromosomes comparing expressing to non-expressing cells (purple bar). Error bars are accumulated measured uncertainty in the experiments. Dashed line indicates 1-fold change (no change).

CHAPTER 5

PHENOTYPIC CHARACTERIZATION OF KATANIN P60 IN S2 CELLS

5.1 Summary

In this chapter, I describe the phenotypes observed upon overexpression of human katanin p60 in *Drosophila* S2 cells. These results are preliminary and unpublished.

5.2 Introduction

We were expecting to observe a stronger phenotype of chromosome misalignment in cells expressing soluble or Mis12-tagged katanin p60 WT or S131A variants. To this end, we attempted a number of experiments.

The first possibility we considered was that hexamer formation was impaired. This could occur because of many reasons. The first being that endogenous Mis12 and Mis12-p60 constructs were competing for assembly at the kinetochore. Further, Mis12 forms homotetramers. Knockdown of Mis12 via RNAi-mediated depletion is suboptimal because the desired target mRNA sequence must be at least 500 nucleotides for effective knockdown, therefore we did not attempt this. Another reason could be that the endogenous Drosophila katanin p60 was forming heterohexamers with the tethered human katanin p60 via the AAA+ domain. This could occur during both metaphase and anaphase. The Aurora kinase regulation site on Drosophila katanin p60 did not show up in

the published literature, but we have obtained prediction results from GPS 3.0, predicting an Aurora B kinase phosphorylation site that corresponds to Ser131.

5.3 Results

5.3.1 Increasing the dose of MG132 does not increase chromosome misalignment.

We had optimized the dose of MG132, and had then considered increasing it to see if we could get greater misalignment. To this end, I treated cells with two doses of MG132 - 10uM and 20uM, but did not see enough of a significant difference to warrant changing the concentration of MG132 for our following experiments.

5.3.2 Knockdown of endogenous *Drosophila* katanin via RNAi does not increase chromosome misalignment in Mis12p60S131A expressing cells

Using previously published sequences from the Sharp and Rogers labs, we generated dsRNA against *Drosophila* katanin (Zhang et al., 2007; Grode and Rogers, 2015). Stable cell lines of Mis12p60S131A were treated with 25ug/ml DmKat60 dsRNA for four days, and induced overnight on the third day. Cells were treated with control dsRNA or Dmkat60 dsRNA, fixed and processed for the chromosome misalignment assay. A sample of the cells was used to confirm protein depletion by Western Blot, and we obtained 80% knockdown for the cells. However, we did not observe a dramatic difference in chromosome misalignment.

CHAPTER 6

CLOSING REMARKS, DISCUSSION, AND FUTURE DIRECTIONS

6.1 Closing Remarks

The intracellular spatiotemporal dynamics of microtubules must change in order to carry out diverse cellular functions throughout the lifetime of the cell. However, current tools preclude our understanding of the regulation of individual networks. Katanin p60, a microtubule-severing enzyme and regulator of microtubule dynamics, localizes to many cellular compartments – although not all location-specific functions have been elucidated. In this dissertation, we utilize the microtubule-severing enzyme katanin p60 to create a tool that localizes this protein to a site of interest, such as the kinetochore, to obtain local severing. Such a tool could be used to identify other physiological roles of katanin p60, when used in a rescue experiment.

6.2 Discussion

Cells display a diversity of microtubule networks - even within the same cell or cellular apparatus. The filaments within these networks can have different lengths, stabilities, and crosslinkers. The organization of the filaments within the networks of a single cell can be parallel bundled, antiparallel bundled, astral, and disorganized. Each of these network organizations can perform a different function locally, and the disruption of an individual microtubule network, while leaving the rest intact, is a desirable experimental tool. Here, we have created and quantitatively characterized a new microtubule-disruption tool based on katanin p60 specifically localizing to a region of the cell. We have localized

human katanin p60 to the kinetochore of *Drosophila* S2 cells as a first test. We showed that soluble human katanin p60 can significantly reduce the polymer density of fly microtubules, through a potential combination of severing and depolymerization. This data is consistent with a microtubule-removing tool that is usable in a cross-species environment. We demonstrated that Mis12, a kinetochore complex protein, can be used to tether and localize katanin p60 to the kinetochores during mitosis, and sequester katanin p60 to the nucleus during interphase.

When placed at the kinetochore, human katanin p60 can be turned off by the Aurora B kinase phosphorylation site at S131. The inhibition can be overridden using the non-phosphorylatable mutant S131A, and katanin p60 is shown to be active at the kinetochore by causing a significant increase in chromosome misalignment.

Our tool is broadly applicable to many cellular compartments by exploiting marker proteins for localization. Through the initial characterization of this tool during mitosis, we have uncovered important properties that should be considered while designing such tools. For instance, a tau-katanin p60 or tau-spastin fusion could specifically target and enhance severing of axonal microtubules. A fusion with an Endoplasmic Reticulum (ER) surface protein could address the importance of the release of non-centrosomal microtubules that are nucleated at the ER. An added benefit of our copper-sulfate inducible expression is that protein expression levels can be titrated by controlling the amount of

copper sulfate added. For experiments examining interphasic processes, katanin p60 could be induced at low levels of expression, yet the targeted katanin p60 tool could have a locally high concentration to facilitate assembly and carry out its microtubule-disrupting function.

Our study has revealed new insight into the function of katanin p60 and its effects in mitosis in S2 cells. Specifically, we found that human katanin p60 was inhibited when near the chromosomes; the most likely mechanism is through inhibition via Aurora B kinase, similar to the *Xenopus* katanin p60 (Loughlin et al., 2011). The presence of additional, active katanin p60 does not affect spindle length in S2 cells. This is distinct from previous work that reported katanin p60 was important for meiotic spindle scaling in *Xenopus* egg extracts (Loughlin et al., 2011). A caveat of this result is that we did not obtain sufficient transfected cells expressing human katanin p60 arrested in metaphase in order for us to measure spindle lengths there. Our results support prior findings that Aurora B kinase activity inhibits katanin p60 (Loughlin et al., 2011); our new findings suggest that spindle length is predominantly regulated by other mechanisms in S2 cells since soluble katanin p60 over-expression (either WT or S131A) did not change spindle length (Figure 11, Figure 12).

Another interesting finding is that, when katanin is placed at the kinetochores by Mis12, there is no significant qualitative effect on either kinetochore fibers, or gross morphological or dynamical changes to the spindle. This result is similar to a prior study on a different, highly potent microtubule destabilizer, Kif2C, a

kinesin-family microtubule depolymerizing enzyme (Manning et al., 2007). This prior work showed that ectopic localization of Kif2C to the centrosome was able to alter the dynamics of kinetochore microtubules - specifically, flux was depressed, and kinetochore fiber turn-over was enhanced (Manning et al., 2007). Sister chromatid spacing and coordination was also adversely affected by excess depolymerizing kinesin at the centrosome (Manning et al., 2007). This paper showed that the localization of a potent microtubule destabilizer near the microtubule-chromosome connection point can have subtle effects (Manning et al., 2007). However, in our study, we did not observe increases in interkinetochore distances using staining of the kinetochore marker Knl1 in our immunofluorescence experiments.

We tried many approaches to obtain greater chromosome misalignment. The RNAi experiments gave us 80% knockdown in the Mis12p60S131A background, but did not give us a dramatic increase in misalignment. We tried adding linker sequences such as titin PEVK, a 1000 amino acid linker, between Mis12 and p60 At first, the protein bands were detectable by Western blot in the first round, but were not observed upon further selection. We used a shorter 50 aa disordered (GGGGS)x10 domain linker between Mis12 and katanin p60 but did not observe dramatic increases in phenotype. Further, the expression of soluble p60 WT or S131A would address the question of defective orientation of katanin p60, because the soluble p60 would not be physically constrained. We saw some increase in misalignment between the Mis12p60S131A and the soluble p60 S131A, and is a likely outcome of tethering. We did not have a Mis12 knockout

cell line to evaluate its effects on misalignment. This can be attempted in the future using CRISPR to knock out the endogenous Mis12.

Many studies of katanin p60 severing activity and regulation have been performed *in vitro* by our group and others (Vale, 1991; McNally and Vale, 1993; Zhang et al., 2011; Bailey et al., 2015; Díaz-Valencia et al., 2011). Whereas previous *in vivo* studies on katanin p60 have been largely limited to whole cell knockdowns (Zhang et al., 2007, 2011; Grode and Rogers, 2015; Jiang et al., 2017), a targeting tool for katanin p60 could enable quantitative biochemical and biophysical measurements in live cells with control over local concentration of katanin p60, *in situ*. Future experiments will permit a high degree of spatial and temporal control of katanin inside living cells.

6.3 Future directions

6.3.1 What does the Mis12p60 pulldown tell us?

It is thought that katanin p60 is operating at the kinetochore to sever or depolymerize microtubules (Zhang et al., 2007). We currently do not know what regulates katanin function at the kinetochore to activate it during anaphase, and drive Pacman flux. The ability to tether katanin to Mis12 at the kinetochore positions us for a pulldown experiment followed up with protein sequencing to identify interacting partners of katanin p60. Such an assay can be extended to other physiologically relevant sites within the cell.

Cheung et al. (2016) have obtained pulldown and mass spectrometry data for each of the katanin p60 and p80 isoforms using stable HeLa cell lines. Their

method allows researchers to create a katanin p60-knockdown background and selective expression of katanin can occur in the desired cellular compartment and cell line. This provides us a starting point to understand the unique regulation of katanin at known sites and processes such as cell migration and cytokinesis. Previous studies of katanin were limited to knockdowns and transient expression systems (Charafeddine et al., 2015; D. Zhang et al., 2011, 2007). Now, it is possible to make stable cell lines with low or inducible katanin expression without getting severe destruction of interphase microtubules.

6.3.2 Which regions are interesting?

GFP-tubulin cells that have been CRISPRed to knock out the endogenous katanin p60 can be coated on coverslips for imaging. I will target the kinetochores through the Nuf2 protein, Golgi through AKAP450, the inner leaflet of the plasma membrane with a CAAX domain, nuclear membrane through lamins, and focal adhesions. These studies would yield further insight into the local partners and spatial regulation of katanin p60.

6.3.3 Second and third generation of the localized microtubule-severing tool

The targeting system can be used with chemical genetics for knock-sideways experiments that would allow rapid sequestration of katanin p60 to a desired location. The FKBP-FRB tag system is frequently used for these experiments. The targeting system can be further developed with optogenetics to gain tighter spatial and temporal control over katanin. I can use a photocaged dimerizer system created by Lampson and Chenoweth labs. For both schemes, stable cell

lines can be recovered after selection of cells expressing low levels of katanin p60. The katanin p60 in these cells can be redistributed to obtain high local concentrations at sites of interest.

These systems have many advantages listed below: (1) exogenous proteins can be expressed at lower levels, so that large-scale destruction of the microtubule network does not occur; (2) the design of this system is modular; (3) chimeric proteins for targeting cellular compartments can be made without disrupting their function; (4) many of the constructs are available through plasmid repositories such as Addgene.

Specific spatial activation of the photocaged dimerizer will be achieved by placing a mask with a pinhole after the 405 nm laser in the light path of our TIRF microscope. Microtubules can be damaged upon prolonged imaging, so I will run the appropriate controls before addition of the photocaged dimerizer. I could create constructs of katanin with a Haloenzyme tag to bind to one end of the small molecule. The second side will bind specifically to a known protein that localizes to the site of interest. This protein will be tagged with *E. coli* Dihydrofolate reductase enzyme (eDHFR). After incubation of the cells with the soluble and photosensitive dimerizer NVOC-TMP-Halotag, the NVOC photocage is cleaved after a 405 nm pulse, unmasking the Trimethoprim (TMP) that can now freely bind to eDHFR.

Alternatives described in the paper for the HaloTag (SNAP tag), DHFR- TMP (glucocorticoid receptor-dexamethasone) and NVOC (red-shifted coumarin-

based photocage) can be used, but since then the Lampson and Chenoweth labs have derived a second generation of dimerizers that can also be considered. The ability of this system to localize to kinetochores, centromeres, mitochondria and centrosomes has been validated (Ballister et al., 2014).

6.3.4 A fluorescence-based unfolding reporter of katanin activity

It is known that the microtubule code dictates interactions with microtubule-associated proteins (Honda et al., 2017; Janke, 2014). It was observed that the knockdown of katanin in *Tetrahymena* led to an increase in acetylated and polyglutamylated microtubules (Sharma et al., 2007). These modifications are primarily on the C-terminal tail, with the sole exception of acetylation which is likely to occur inside the microtubule lumen. Unpublished data from our lab finds that severing activity of katanin is influenced by these posttranslational modifications (Bailey et al., 2015). Subtilisin treatment of microtubules to cleave the C-terminal tail of tubulin negatively affects katanin-mediated severing (Bailey et al., 2015). The solved solution NMR structure of spastin revealed a hexameric ring with a pore in the center - typical of AAA+ ATPases – that is thought to be important for threading the C-terminal tail through the pore (Roll-Mecak & Vale, 2008). The charged residues are thought to be responsible for the differences observed with various tubulin PTMs via their interaction with the residues in the AAA+ pore. Recently, the X-ray crystal structure of the katanin p60 monomer from *C. elegans* was solved by Zehr et al. (2017), and the data used to solve the cryo-EM Structure of the hexamer.

We still do not know whether katanin-mediated microtubule destruction occurs through the wedge or threading model (Vale, 2000). We know that the tubulin released upon severing can be incorporated back into polymerizing microtubules, making it unlikely that the entire subunit is unfolded (Hartman et al., 1998; McNally & Vale, 1993). Zehr et al. (2017) report two different conformations of katanin p60, and hypothesize that ATP-driven switching between the two forms generates a power stroke necessary for tubulin removal, but that does not give us a full understanding of the mechanism of severing.

To this end, we have created a fluorescent-based reporter of severing activity to use for single molecule experiments to identify the number of subunits docking onto each tail. Photobleaching data reveals that the reporter is monomeric as expected. The next step is to standardize the TIRF assay for single molecule experiments. We would first need to observe single molecules that are sufficiently separated. We expect a single-step photobleaching of the TagRFP-CTT protein. Given the stochastic photobleaching of an individual fluorophore molecule, the graph of intensity over time is a step function. When the I(t) is integrated for all the photobleaching fluorophore molecules in the system, this yields an exponential decay curve, confirming single TagRFP-CTTs per imaging field. Photobleaching experiments repeated with GFP-katanin would be done to determine the number of steps required to photobleach GFP. I would need to repeat this with each C-terminal tail and the no-tail control.

In bulk fluorimetry assays, we can obtain the binding coefficients of GFP-katanin binding to the TagRFP C-terminal tails. The association rate k_{ON} of GFP-katanin with the C-terminal tails can be determined using a saturation binding experiment. We would use the dilution method to determine the half-life of dissociation and its reciprocal, k_{OFF} to determine if the red fluorescence decreases over time as a function of katanin concentration for each of the tails. These experiments will be run with or without katanin or C-terminal tail, and observe how the nucleotide energy source affects the rate of unfolding of TagRFP-T. We can expect little to no change in the fluorescence of TagRFP-T in the ATPγS or no ATP conditions.

We created the microtubule-disruption tool using a microtubule-severing enzyme, katanin p60 to circumvent the effects of global loss of microtubule polymer due to high-level overexpression of katanin p60. Large scale severing of microtubules was prevented by specific localization of katanin p60 to a target region. Here, as a first test, I chose to localize the katanin p60 to the *Drosophila* kinetochore in S2 cells using Mis12. We reasoned that localizing katanin p60 to the kinetochores, where it could directly affect microtubule attachment to the chromosomes, could serve as a proof-of-concept. We were able to demonstrate this proof-of-concept in this dissertation.

APPENDIX A

GIBSON CLONING PROTOCOL

The goal is to generate regions of overlap between the vector and the insert, which will be recognized by the enzymes in the Gibson CBA (Chew Back and Anneal) method.

Primer design:

1. Design primers with 20nt overlap with the vector+20nt of the sequence to be amplified. The Tm of the 20nt overlap should be as close to 50^{o}C as possible.
2. Follow the usual rules for designing primers
3. Run the overlap sequence through IDT's Oligo Analyzer to ensure that the overlap region is free of secondary structure. This is very important!
4. Check the affinity of the primer set for primer dimer formation. This way, it will have more affinity for the actual sequence to be amplified than each other.
5. Run *in silico* PCRs and assembly. If your design works or needs to be tweaked, you will know immediately.

Procedure:

1. Amplify the insert and gel-purify the PCR product. Use a high fidelity polymerase and do not exceed 25 cycles.
2. Digest 1ug of the vector with one or two restriction enzymes near the site of insertion, and gel purify the vector. If you don't have restriction sites, use PCR to amplify the vector.
3. Elute the products are eluted in 30ul water at 50^{o}C.
4. Take the OD of all the products after gel purification and make a 1:1 equimolar mix of the construct and insert (0.02pmol of each is preferred). You can also try a reaction with 1:3 to see which one gives you better results. All of this has to fit in 5ul of DNA.
5. Run the Gibson program on the PCR machine. 2-4 fragments (50^{o}C/15min); more than 4 (50^{o}C/60min)

Notes:

1. I made the Gibson mix according to the paper, and tested it out with a positive control. NEB sells this as part of their Gibson kit.
2. The Barrick lab figured out what NEB was using, and it's basically two fragments of pUC19 split along an ampicillin resistance gene. I made a bunch of this, and it's in the -20^{o}C ready to go. I use 5ul of this mix for the control reaction.
3. You can use this control to QC the Gibson mix.
4. Precautions: The assembly is extremely salt sensitive, and you can only add 5ul of DNA.

5. Transformation: Dilute 1ul in 5ul of water, and use all of it to transform a 50ul aliquot of DH5alpha competent cells. The alternative is to clean up the PEG because it's toxic to the bacteria.

APPENDIX B

DIRECTIONAL RESTRICTION CLONING

1. Choose RE sites that are present in the vector of choice but absent in the insert
2. Append these to the forward and reverse primers along with the necessary overhangs to promote efficient cutting (refer to the NEB website for the minimum number of nucleotides needed for each enzyme)
3. To ensure that the correct reading frame is preserved, simulate the PCR, digest and ligation in SerialCloner or SnapGene
4. Perform vector dephosphorylation (if necessary) and ligation as described below.

1. Dephosphorylation with CIP

1. The goal is to reduce the background of vector self-ligation when combining vector and an insert

2. Vector-insert ligation

1. Ensure the vector has been dephosphorylated before performing this ligation
2. Maximum volume is 10ul of mix.
3. You can only use 5ul per transformation of cells (50ul)
4. Use molar ratios of 1:1 and 1:3. If the insert is very small, use 1:5.
5. Let the total DNA in the mix be anywhere between 20-100ng

3. Self-ligation

1. Just the near-opposite of vector-insert ligation
2. Dilute the products as much as possible so that self-ligation is favored at low DNA concentrations
3. Very small amounts of T4 DNA ligase are needed for the ligation to be efficient
4. This ligation is also faster and can be finished at room temperature in an hour (5min if using the quick ligase mix from NEB)

Linear DNA	10-50ng
10x T4 DNA ligase buffer	5ul
T4 DNA ligase	5units **less than 0.1ul**
Water, nuclease-free	to 50ul

5. Mix thoroughly and incubate at 20^{o}C/10min for sticky ends or 20^{o}C/1hr for blunt ends
6. Heat inactivate the T4 ligase at 65^{o}C/10min
7. Transform 5ul into DH5alpha cells

APPENDIX C

IMMUNOFLUORESCENCE PROTOCOL FOR S2 CELLS

1. Induce 500ul of cells overnight in a 35mm dish containing 500uM copper sulphate and 1.5ml S2 media. Seal the edges with parafilm and store in the incubator at room temperature.
2. Allow cells to flatten down on a ConA-coated coverslip for 20min.
3. Plate them at about ½ the density that you would otherwise. You do not want the cells to overlap or touch.
4. Wash cells in 1x BRB-80, vacuum aspirate the excess liquid. Do this quickly using the vacuum pump to remove the buffer between washes. Do not allow the cells to dry out otherwise the spindles will look less than ideal.
5. Fix with 1-2ml of freshly mixed paraformaldehyde (3.12 ml 33% Formaldehyde with 6.78 ml BRB-80), incubate 10 minutes
6. Ensure that the coverslip and the bottom of the dish are completely covered and do not dry out. Remove fixative with the vacuum aspirator. Permeabilize with PBS+ 1%Triton for 8 minutes.
7. Wash 2x with PBS+ 0.1% Triton.
8. Carefully transfer the coverslips out of the dish onto a prepared parafilm sheet in a large petri dish using forceps.
9. Make sure the parafilm is labeled so that you can easily tell your coverslips apart. As soon as the coverslip is on the parafilm cover it with PBS + 0.1% Triton. This counts as the 3rd wash.
10. Cover with Boiled Donkey Serum and incubate for 45 minutes at room temperature
11. While this is incubating set up your primary and secondary antibodies in Boiled Donkey Serum using the specific dilution factors for each antibody you are using. Secondary antibodies are always used at 1:200. 500ul of Primary and Secondary are adequate for 3 coverslips.
12. Remove the block off using a vacuum aspirator by going around the edges of the coverslip. Then apply 150ul of Primary antibody.
13. Incubate for 1 hour at room temperature or overnight in a humidity chamber at 4^{o}C.
14. Wash 3 times with a five-minute incubation between washes using PBS+0.1%Triton
15. After the final wash carefully aspirate off all of the PBS and then apply 150ul of Secondary antibody (make sure that your secondaries match your primaries!)
16. Incubate for 1 hour at room temperature or overnight in a humidity chamber at 4^{o}C. A minimum of 40 minutes is okay.
17. Aspirate off the antibody and wash 3x with PBS +0.1% Triton (5 minute incubations)
18. Add DAPI in boiled donkey serum at a concentration of 1:1000, 10min/RT.

19. Aspirate off the DAPI and wash 3x with PBS +0.1% Triton (5 minute incubations)
20. Cover with PBS +0.1% triton (bottle) while you lay out and label the slides.
21. Put 7ul of mounting media on your slide, and carefully place your coverslip face down in the mounting media
22. Repeat this for all the remaining coverslips.
23. After a few minutes, place a dot of nailpolish on each corner of the coverslip. Allow it to dry.
24. Continue to carefully line the outside of each coverslip with nailpolish, allow to dry, and store at 4^{o}C in a slide box.

APPENDIX D

SITE-DIRECTED MUTAGENESIS PROTOCOL

Control reaction

10x Reaction buffer	2.5 µl
Control template	1 µl
Control primer mix	1 µl
dNTP mix (10mM)	1 µl
Quikchange Lightning Multisite enzyme blend	1 µl
Molecular Biology H_2O	18.5 µl
Total	25 µl

Mutagenesis reaction

10x Reaction buffer	2.5 µl	
Template	1.12 µl	50ng for <5kb, 100ng for >5kb
Forward Primer	0.8 µl	100ng each for 1-3 primers, 50ng each for 4-5 primers
Reverse Primer	0.8 µl	
QuikSolution	0.75 µl	For templates >5kb, also add 0-0.75µl of QuikSolution to the reaction. Titrate to determine optimal concentration
dNTP mix	1 µl	
Quikchange Lightning Multisite enzyme blend	1 µl	
Molecular Biology H_2O	17.03 µl	
Total	25 µl	

APPENDIX E

STATEMENT FROM THE AUTHOR

Under the advice of the dissertation committee, I, Siddheshwari Advani, the author and copyright holder of this dissertation do hereby state that: Siddheshwari Advani was a graduate student in the lab of Dominique Alfandari, Ph.D., from June 2012-August 2015. Advani successfully passed the MCB Original Research Proposal examination in May 2013. Advani achieved Ph.D. candidacy in August 2014, and her dissertation work was titled “Role of ADAM13 and MDC13 in the gastrulation of *Xenopus laevis*”. This work is unpublished and is not included in this dissertation, as it was work done prior to achieving candidacy in the lab of Jennifer Ross, Ph.D.

Advani acknowledges and thanks Dominique Alfandari, Ph.D., and Helene Cousin, Ph.D. for the training received in the Alfandari lab.

BIBLIOGRAPHY

Arnal, I., & Wade, R. H. (1995). How does Taxol stabilize microtubules? Current Biology, 5(8), 900–908. https://doi.org/10.1016/S0960-9822(95)00180-1

Bailey, M. E., Sackett, D. L., & Ross, J. L. (2015). Katanin Severing and Binding Microtubules Are Inhibited by Tubulin Carboxy Tails. Biophysical Journal, 109(12), 2546–2561. https://doi.org/10.1016/j.bpj.2015.11.011

Ballister, E. R., Aonbangkhen, C., Mayo, A. M., Lampson, M. A., & Chenoweth, D. M. (2014). Localized light-induced protein dimerization in living cells using a photocaged dimerizer. Nature Communications, 5, 5475. https://doi.org/10.1038/ncomms6475

Ballister, E. R., Ayloo, S., Chenoweth, D. M., Lampson, M. A., & Holzbaur, E. L. (2015). Optogenetic control of organelle transport using a photocaged chemical inducer of dimerization. Current Biology : CB, 25(10), R407–R408. https://doi.org/10.1016/j.cub.2015.03.056

Ballister, E. R., Riegman, M., & Lampson, M. A. (2014). Recruitment of Mad1 to metaphase kinetochores is sufficient to reactivate the mitotic checkpoint. The Journal of Cell Biology, 204(6), 901–908. https://doi.org/10.1083/jcb.201311113

Charafeddine, R. A., Makdisi, J., Schairer, D., O'Rourke, B. P., Diaz-Valencia, J. D., Chouake, J., … Sharp, D. J. (2015). Fidgetin-Like 2: A Microtubule-Based Regulator of Wound Healing. The Journal of Investigative Dermatology, 135(9), 2309–2318. https://doi.org/10.1038/jid.2015.94

Cheeseman, I. M., Anderson, S., Jwa, M., Green, E. M., s Kang, J., Yates, J. R., … Barnes, G. (2002). Phospho-regulation of kinetochore-microtubule attachments by the Aurora kinase Ipl1p. Cell, 111(2), 163–72.

Cheung, K., Senese, S., Kuang, J., Bui, N., Ongpipattanakul, C., Gholkar, A., … Torres, J. Z. (2016). Proteomic Analysis of the Mammalian Katanin Family of Microtubule-severing Enzymes Defines Katanin p80 subunit B-like 1 (KATNBL1) as a Regulator of Mammalian Katanin Microtubule-severing. Molecular & Cellular Proteomics : MCP, 15(5), 1658–69. https://doi.org/10.1074/mcp.M115.056465

Díaz-Valencia, J. D., Morelli, M. M., Bailey, M., Zhang, D., Sharp, D. J., & Ross, J. L. (2011). Drosophila katanin-60 depolymerizes and severs at microtubule defects. Biophysical Journal, 100(10), 2440–9. https://doi.org/10.1016/j.bpj.2011.03.062

Frickey, T., & Lupas, A. N. (2004). Phylogenetic analysis of AAA proteins. Journal of Structural Biology, 146(1–2), 2–10. https://doi.org/10.1016/j.jsb.2003.11.020

Fu, W., Wu, H., Cheng, Z., Huang, S., & Rao, H. (2018). The role of katanin p60 in breast cancer bone metastasis. Oncology Letters, 15(4), 4963–4969. https://doi.org/10.3892/ol.2018.7942

Gibson, D. G. (2011). Methods in Enzymology. Methods in Enzymology, 498, 349–361. https://doi.org/10.1016/B978-0-12-385120-8.00015-2

Gibson, D. G., Young, L., Chuang, R.-Y., Venter, C. J., III, C. A., & Smith, H. O. (2009). Enzymatic assembly of DNA molecules up to several hundred kilobases. Nature Methods, 6(5), nmeth.1318. https://doi.org/10.1038/nmeth.1318

Gigant, B., Wang, C., Ravelli, R. B., Roussi, F., Steinmetz, M. O., Curmi, P. A., … Knossow, M. (2005). Structural basis for the regulation of tubulin by vinblastine. Nature, 435(7041), 519–22. https://doi.org/10.1038/nature03566

Gomes, J.-E., Tavernier, N., Richaudeau, B., Formstecher, E., Boulin, T., Mains, P. E., … Pintard, L. (2013). Microtubule severing by the katanin complex is activated by PPFR-1–dependent MEI-1 dephosphorylation. The Journal of Cell Biology, 202(3), 431–439. https://doi.org/10.1083/jcb.201304174

Grode, K. D., & Rogers, S. L. (2015). The Non-Catalytic Domains of *Drosophila* Katanin Regulate Its Abundance and Microtubule-Disassembly Activity. PLOS ONE, 10(4), e0123912. https://doi.org/10.1371/journal.pone.0123912

Han, H., Monroe, N., Votteler, J., Shakya, B., Sundquist, W. I., & Hill, C. P. (2015). Binding of Substrates to the Central Pore of the Vps4 ATPase Is Autoinhibited by the Microtubule Interacting and Trafficking (MIT) Domain and Activated by MIT Interacting Motifs (MIMs). The Journal of Biological Chemistry, 290(21), 13490–9. https://doi.org/10.1074/jbc.M115.642355

Hartman, J. J., Mahr, J., McNally, K., Okawa, K., Iwamatsu, A., Thomas, S., … McNally, F. J. (1998). Katanin, a Microtubule-Severing Protein, Is a Novel AAA ATPase that Targets to the Centrosome Using a WD40-Containing Subunit. Cell, 93(2), 277–87. https://doi.org/10.1016/S0092-8674(00)81578-0

Hartman, J. J., & Vale, R. D. (1999). Microtubule Disassembly by ATP-Dependent Oligomerization of the AAA Enzyme Katanin. Science, 286(5440), 782–785. https://doi.org/10.1126/science.286.5440.782 Hemmerich, P., Weidtkamp-Peters, S., Hoischen, C., Schmiedeberg, L., Erliandri, I., & Diekmann, S. (2008). Dynamics of inner kinetochore assembly and maintenance in living cells. The Journal of Cell Biology, 180(6), 1101–14. https://doi.org/10.1083/jcb.200710052

Honda, Y., Tsuchiya, K., Sumiyoshi, E., Haruta, N., & Sugimoto, A. (2017). Tubulin isotype substitution revealed that isotype composition modulates microtubule dynamics in *C. elegans* embryos. J Cell Sci, jcs.200923. https://doi.org/10.1242/jcs.200923

Hori, T., Haraguchi, T., Hiraoka, Y., Kimura, H., & Fukagawa, T. (2003). Dynamic behavior of Nuf2-Hec1 complex that localizes to the centrosome and centromere and is essential for mitotic progression in vertebrate cells. Journal of Cell Science, 116(Pt 16), 3347–62. https://doi.org/10.1242/jcs.00645

Janke, C. (2014). The tubulin code: molecular components, readout mechanisms, and functions. The Journal of Cell Biology, 206(4), 461–72. https://doi.org/10.1083/jcb.201406055

Jiang, K., Rezabkova, L., Hua, S., Liu, Q., Capitani, G., Altelaar, M. A., … Akhmanova, A. (2017). Microtubule minus-end regulation at spindle poles by an ASPM-katanin complex. Nature Cell Biology, 19(5), 480–492. https://doi.org/10.1038/ncb3511

Jordan, M., & Wilson, L. (2004). Microtubules as a target for anticancer drugs. Nature Reviews Cancer, 4(4), nrc1317. https://doi.org/10.1038/nrc1317

Kline, S., Cheeseman, I., & Hori, T. (2006). The human Mis12 complex is required for kinetochore assembly and proper chromosome segregation.

Kuo, T.-C., Li, L.-W., Pan, S.-H., Fang, J.-M., Liu, J.-H., Cheng, T.-J., … Yang, P.-C. (2016). Purine-Type Compounds Induce Microtubule Fragmentation and Lung Cancer Cell Death through Interaction with Katanin. Journal of Medicinal Chemistry, 59(18), 8521–8534. https://doi.org/10.1021/acs.jmedchem.6b00797

Loughlin, R., Wilbur, J. D., McNally, F. J., Nédélec, F. J., & Heald, R. (2011). Katanin Contributes to Interspecies Spindle Length Scaling in Xenopus. Cell, 147(6), 1397–407. https://doi.org/10.1016/j.cell.2011.11.014

Maldonado, M., & Kapoor, T. M. (2011). Constitutive Mad1 targeting to kinetochores uncouples checkpoint signaling from chromosome biorientation. Nature Cell Biology, 13(4), ncb2223. https://doi.org/10.1038/ncb2223

Manning, A. L., Ganem, N. J., Bakhoum, S. F., Wagenbach, M., Wordeman, L., & Compton, D. A. (2007). The Kinesin-13 Proteins Kif2a, Kif2b, and Kif2c/MCAK Have Distinct Roles during Mitosis in Human Cells. Molecular Biology of the Cell, 18(8), 2970–2979. https://doi.org/10.1091/mbc.E07-02-0110

McNally, F. J., & Thomas, S. (1998). Katanin Is Responsible for the M-Phase Microtubule-severing Activity in Xenopus Eggs. Molecular Biology of the Cell, 9(7), 1847–61. https://doi.org/10.1091/mbc.9.7.1847

McNally, F. J., & Vale, R. D. (1993). Identification of katanin, an ATPase that severs and disassembles stable microtubules. Cell, 75(3), 419–29. https://doi.org/10.1016/0092-8674(93)90377-3

Mitchison, T., & Kirschner, M. (1984). Dynamic instability of microtubule growth. Nature, 312(5991), 312237a0. https://doi.org/10.1038/312237a0

Monroe, N., Han, H., Gonciarz, M. D., Eckert, D. M., Karren, M. A., Whitby, F. G., … Hill, C. P. (2014). The oligomeric state of the active Vps4 AAA ATPase. Journal of Molecular Biology, 426(3), 510–25. https://doi.org/10.1016/j.jmb.2013.09.043

Monroe, N., & Hill, C. P. (2016). Meiotic Clade AAA ATPases: Protein Polymer Disassembly Machines. Journal of Molecular Biology, 428(9 Pt B), 1897–911. https://doi.org/10.1016/j.jmb.2015.11.004

Panda, D., Jordan, M., Chu, K., & Wilson, L. (1996). Differential effects of vinblastine on polymerization and dynamics at opposite microtubule ends. The Journal of Biological Chemistry, 271(47), 29807–12.

Peng, W., Lin, Z., Li, W., Lu, J., Shen, Y., & Wang, C. (2013). Structural insights into the unusually strong ATPase activity of the AAA domain of the Caenorhabditis elegans fidgetin-like 1 (FIGL-1) protein. The Journal of Biological Chemistry, 288(41), 29305–12. https://doi.org/10.1074/jbc.m113.502559

Qi, D., & Scholthof, K.-B. G. (2008). A one-step PCR-based method for rapid and efficient site-directed fragment deletion, insertion, and substitution mutagenesis. Journal of Virological Methods, 149(1), 85–90. https://doi.org/10.1016/j.jviromet.2008.01.002

Quintin, S., Mains, P., Zinke, A., & reports, H. A. (2003). The mbk-2 kinase is required for inactivation of MEI-1/katanin in the one-cell Caenorhabditis elegans embryo.

Roll-Mecak, A., & McNally, F. J. (2010). Microtubule-severing enzymes. Current Opinion in Cell Biology, 22(1), 96–103. https://doi.org/10.1016/j.ceb.2009.11.001

Roll-Mecak, A., & Vale, R. D. (2008). Structural basis of microtubule severing by the hereditary spastic paraplegia protein spastin. Nature, 451(7176), 363–7. https://doi.org/10.1038/nature06482

Salinas, S., Carazo-Salas, R. E., Proukakis, C., Cooper, J., Weston, A. E., Schiavo, G., & Warner, T. T. (2005). Human spastin has multiple microtubule-related functions. Journal of Neurochemistry, 95(5), 1411–20. https://doi.org/10.1111/j.1471-4159.2005.03472.x

Sharma, N., Bryant, J., Wloga, D., Donaldson, R., Davis, R. C., Jerka-Dziadosz, M., & Gaertig, J. (2007). Katanin regulates dynamics of microtubules and biogenesis of motile cilia. The Journal of Cell Biology, 178(6), 1065–1079. https://doi.org/10.1083/jcb.200704021

Sharp, D. J., & Ross, J. L. (2012). Microtubule-severing enzymes at the cutting edge. Journal of Cell Science, 125(Pt 11), 2561–9. https://doi.org/10.1242/jcs.101139

Sudo, H., & Maru, Y. (2008). LAPSER1/LZTS2: a pluripotent tumor suppressor linked to the inhibition of katanin-mediated microtubule severing.

Tanaka, T., Rachidi, N., Janke, C., Pereira, G., & Cell, G. M. (2002). Evidence that the Ipl1-Sli15 (Aurora kinase-INCENP) complex promotes chromosome bi-orientation by altering kinetochore-spindle pole connections.

Vale, R. D. (1991). Severing of stable microtubules by a mitotically activated protein in xenopus egg extracts. Cell, 64(4), 827–839. https://doi.org/10.1016/0092-8674(91)90511-V

Vale, R. D. (2000). Aaa Proteins Lords of the Ring. The Journal of Cell Biology, 150(1), F13–F20. https://doi.org/10.1083/jcb.150.1.F13

van Haren, J., Charafeddine, R. A., Ettinger, A., Wang, H., Hahn, K. M., & Wittmann, T. (2018). Local control of intracellular microtubule dynamics by EB1 photodissociation. Nature Cell Biology, 20(3), 252–261. https://doi.org/10.1038/s41556-017-0028-5

Venkei, Z., Przewloka, M. R., Ladak, Y., Albadri, S., Sossick, A., Juhasz, G., … Glover, D. M. (2012). Spatiotemporal dynamics of Spc105 regulates the assembly of the *Drosophila* kinetochore. Open Biology, 2(2), 110032. https://doi.org/10.1098/rsob.110032

Whitehead, E., Heald, R., & Wilbur, J. D. (2013). N-Terminal Phosphorylation of p60 Katanin Directly Regulates Microtubule Severing. Journal of Molecular Biology, 425(2), 214–21. https://doi.org/10.1016/j.jmb.2012.11.022

Ye, A. A., Deretic, J., Hoel, C. M., Hinman, A. W., Cimini, D., Welburn, J. P., & Maresca, T. J. (2015). Aurora A Kinase Contributes to a Pole-Based Error Correction Pathway. Current Biology : CB, 25(14), 1842–51. https://doi.org/10.1016/j.cub.2015.06.021

Ye, X., Lee, Y.-C. C., Choueiri, M., Chu, K., Huang, C.-F. F., Tsai, W.-W. W., … Lin, S.-H. H. (2012). Aberrant expression of katanin p60 in prostate cancer bone metastasis. The Prostate, 72(3), 291–300. https://doi.org/10.1002/pros.21431

Yu, W., Qiang, L., lowska, J., Karabay, A., Korulu, S., & Baas, P. W. (2008). The microtubule-severing proteins spastin and katanin participate differently in the formation of axonal branches. Molecular Biology of the Cell, 19(4), 1485–98. https://doi.org/10.1091/mbc.E07-09-0878

Zehr, E., Szyk, A., Piszczek, G., Szczesna, E., Zuo, X., & Roll-Mecak, A. (2017). Katanin spiral and ring structures shed light on power stroke for microtubule severing. Nature Structural & Molecular Biology, 24(9), 717–725. https://doi.org/10.1038/nsmb.3448

Zhang, D., Grode, K. D., Stewman, S. F., Diaz-Valencia, J. D., Liebling, E., Rath, U., … Sharp, D. J. (2011). *Drosophila* katanin is a microtubule depolymerase that regulates cortical-microtubule plus-end interactions and cell migration. Nature Cell Biology, 13(4), 361–70. https://doi.org/10.1038/ncb2206

Zhang, D., Rogers, G. C., Buster, D. W., & Sharp, D. J. (2007). Three microtubule severing enzymes contribute to the “Pacman-flux” machinery that moves chromosomes. The Journal of Cell Biology, 177(2), 231–42. https://doi.org/10.1083/jcb.200612011

Zhang, H., Aonbangkhen, C., Tarasovetc, E. V., Ballister, E. R., Chenoweth, D. M., & Lampson, M. A. (2017). Optogenetic control of kinetochore function. Nature Chemical Biology, 13(10), 1096–1101. https://doi.org/10.1038/nchembio.2456